Supporting Information

Discovery of a Potent and Selective Covalent Inhibitor of Bruton's Tyrosine Kinase with Oral Anti-Inflammatory Activity

Author list

Mark S. Tichenor[†*], John J.M. Wiener[†], Navin L. Rao[‡*], Charlotte Pooley Deckhut[†], J. Kent Barbay[‡], Kevin D. Kreutter[‡], Genesis M. Bacani[†], Jianmei Wei[†], Leon Chang[†], Heather E. Murrey[‡], Weixue Wang[‡], Kay Ahn[‡], Michael Huber[†], Elizabeth Rex[†], Kevin J. Coe[†], JieJun Wu[†], Mark Seierstad[†], Scott D. Bembenek[†], Kristi A. Leonard[‡], Alec D. Lebsack[†], Jennifer D. Venable[†], James P. Edwards[†]

[†]Janssen Research & Development, 3210 Merryfield Row, San Diego, USA 92121-1126

[‡]Janssen Research & Development, 1400 McKean Road, Spring House, PA, USA 19477-0776

* Correspondence may be addressed to: Mark Tichenor (mticheno@its.jnj.com) and Navin Rao (nrao2@its.jnj.com)

Contents of Supporting Information: **page**

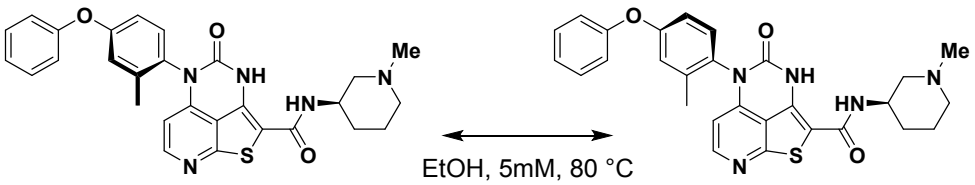

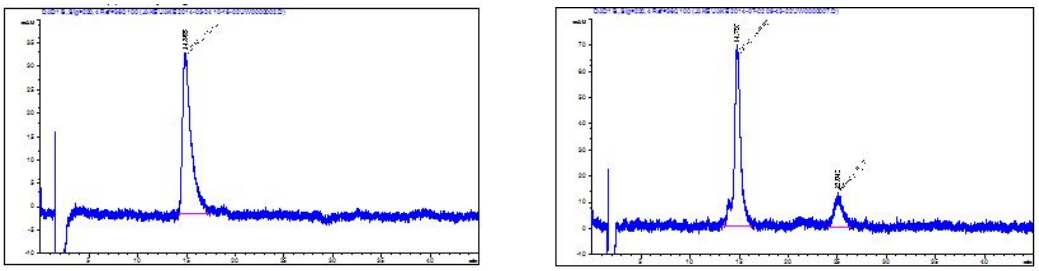

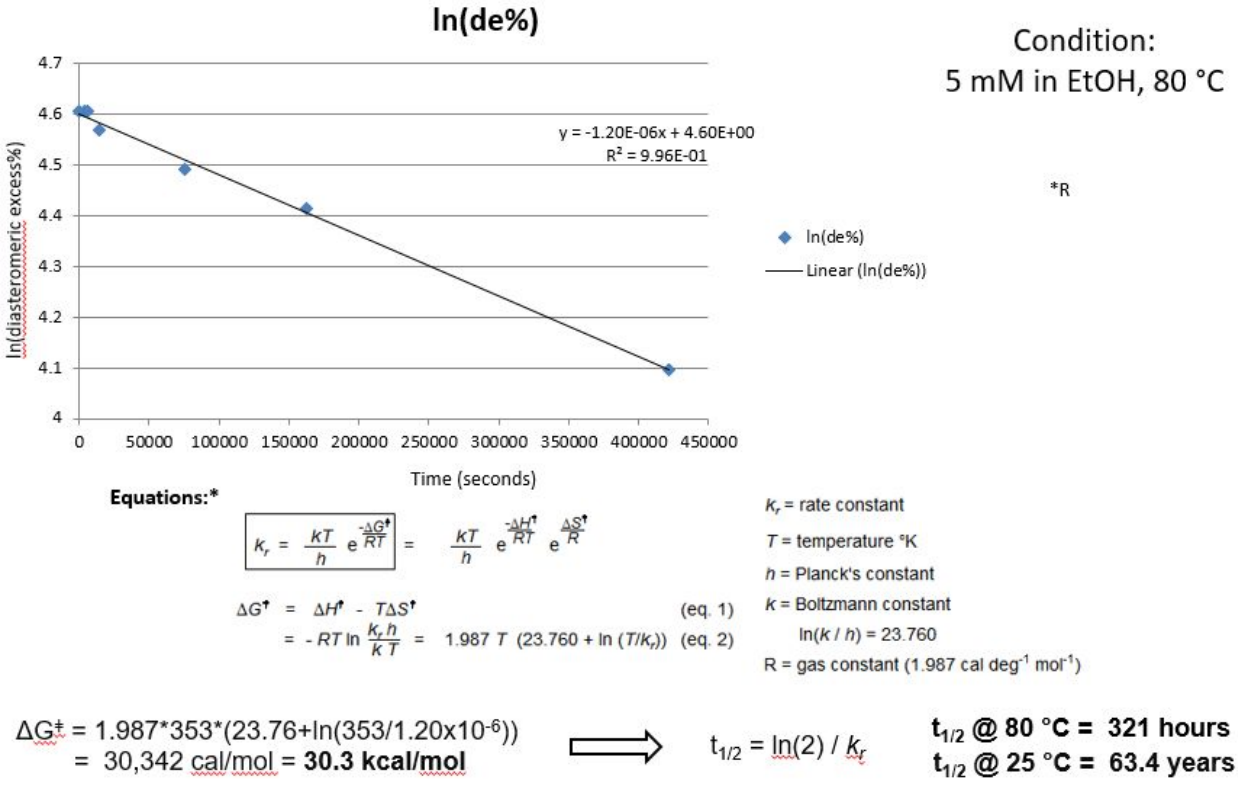

Figure S1. Determination of the atropisomer interconversion barrier for **21**.

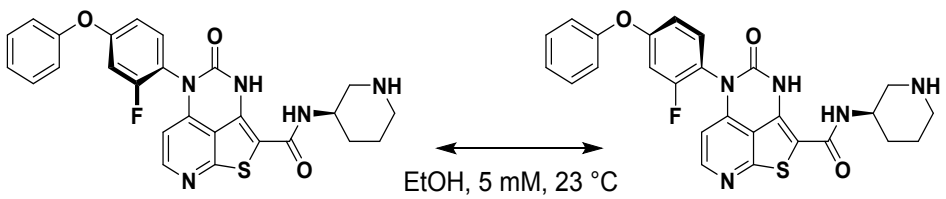

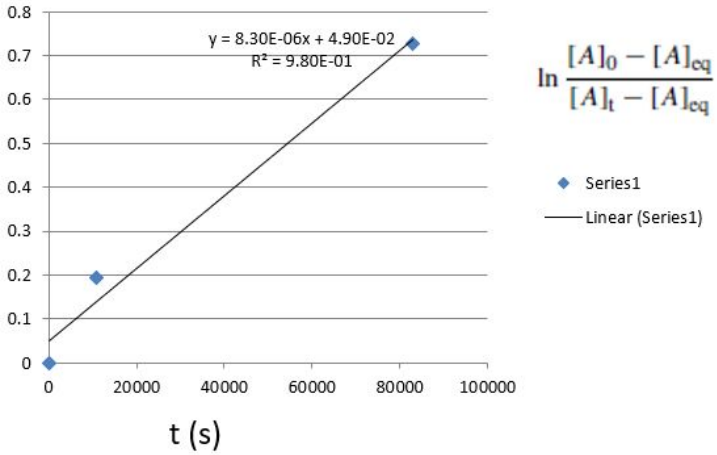

$$\ln \frac{[A]_0 - [A]_{eq}}{[A]_t - [A]_{eq}}$$

From regression plot: k = slope/2 = $4.15*10^{-6}$ s^{-1}

$$\Delta G^{\#} = RT \ln\left(\frac{hk}{\kappa k_B T}\right)$$ = 8.314 J K^{-1} mol^{-1} * 296 K * ln $\frac{(6.626*10^{-34} \text{ J s} * 4.15*10^{-6} \text{ s}^{-1})}{(0.5 * 1.38*10^{-23} \text{ J K}^{-1} * 296 \text{ K})}$

= 101.3 kJ/mol = **24.2 kcal/mol** $t_{1/2}$ at 23 °C = $\frac{\ln 2}{k}$ = 46 hr

Figure S2. Determination of the atropisomer interconversion barrier for **23**.

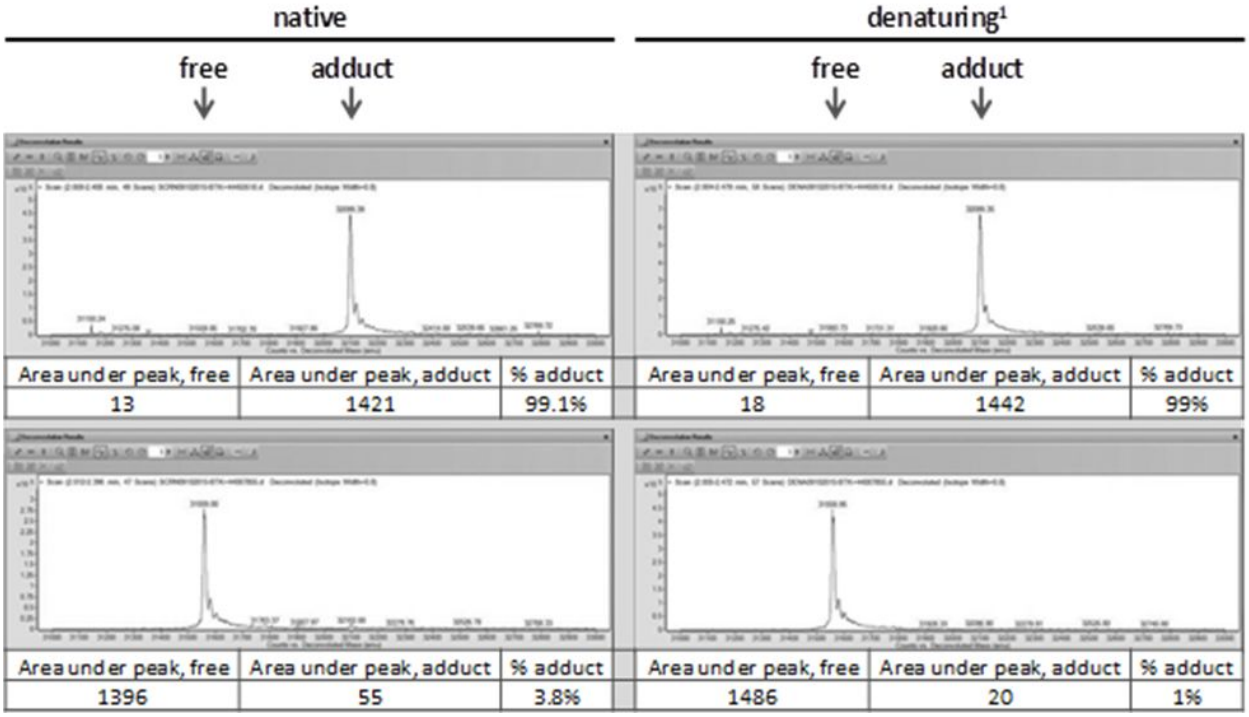

Figure S3. Characterization of BTK inhibitor adduct.

Covalent modification of BTK by compound 27. To verify the covalent mechanism, compound **27** was incubated with BTK protein followed by purification using a C18 reverse phase column under non-denaturing and denaturing conditions (8 M urea, 70 ˚C). The expected mass of free (unmodified) recombinant BTK kinase domain used in this assay is 31,560 Da, and the expected mass of BTK adduct with compound **27** is 32,100 Da. A compound that causes a shift of >95% of BTK to the expected higher molecular weight under native LC/MS conditions and maintains a similar degree (±2-3%) of BTK modification under denaturing conditions is classified as an irreversible covalent inhibitor. The measured mass of the adduct was 32,099.36 Da with abundancies of >98% under both denaturing and non-denaturing conditions, confirming **27** as an irreversible covalent inhibitor of BTK.

Figure S4. Kinase selectivity profile of compound **27** in a human wild type kinase panel at 1 μM (Eurofins).

Assay	Compound **27** % effect at 1 μM
Bruton agammaglobulinemia tyrosine kinase _h_wt_AS_10uMATP	101
BMX non-receptor tyrosine kinase _h_wt_AS_10uMATP	99
tec protein tyrosine kinase (activated)_h_wt_AS_10uMATP	92
lymphocyte-specific protein tyrosine kinase _h_wt_AS_10uMATP	89
v-erb-a erythroblastic leukemia viral oncogene homolog 4_h_wt_AS_10uMATP	86
TXK tyrosine kinase _h_wt_AS_10uMATP	79
lymphocyte-specific protein tyrosine kinase (activated)_h_wt_AS_10uMATP	75
Gardner-Rasheed feline sarcoma viral (v-fgr) oncogene homolog_h_wt_AS_10uMATP	63
v-raf-1 murine leukemia viral oncogene homolog 1_h_wt_AS_10uMATP	62
hemopoietic cell kinase _h_wt_AS_10uMATP	57
c-src tyrosine kinase _h_wt_AS_10uMATP	57
fms-related tyrosine kinase 4_h_wt_AS_10uMATP	48
PTK6 protein tyrosine kinase 6_h_wt_AS_10uMATP	47
epidermal growth factor receptor _h_wt_AS_10uMATP	37
fyn-related kinase _h_wt_AS_10uMATP	37
v-abl Abelson murine leukemia viral oncogene homolog 2 _h_wt_AS_10uMATP	36
FYN oncogene related to SRC, FGR, YES_h_wt_AS_10uMATP	35
v-yes-1 Yamaguchi sarcoma viral related oncogene homolog _h_wt_AS_10uMATP	35
B lymphoid tyrosine kinase_h_wt_AS_10uMATP	32
serine/threonine kinase 17a_h_wt_AS_10uMATP	28
receptor-interacting serine-threonine kinase 2_h_wt_AS_10uMATP	27
EPH receptor B2_h_wt_AS_10uMATP	24
PAS domain containing serine/threonine kinase _h_wt_AS_10uMATP	22
v-src sarcoma viral oncogene homolog_h_wt_AS_10uMATP	20
spleen tyrosine kinase _h_wt_AS_10uMATP	19
Cyclin-dependent kinase 7 / cyclinH / MAT_h_wt_AS_10uMATP	18
interleukin-1 receptor-associated kinase 1_h_wt_AS_10uMATP	18

ribosomal protein S6 kinase, 90kDa, polypeptide 2 _h_wt_AS_10uMATP	17
serine/threonine kinase 33_h_wt_AS_10uMATP	17
kinase insert domain receptor_h_wt_AS_10uMATP	16
dystrophia myotonica-protein kinase _h_wt_AS_10uMATP	16
EPH receptor A2 _h_wt_AS_10uMATP	15
tyrosine kinase, non-receptor, 2 _h_wt_AS_10uMATP	13
hemopoietic cell kinase (activated)_h_wt_AS_10uMATP	13
aurora kinase C_h_wt_AS_10uMATP	13
SFRS protein kinase 3_h_wt_AS_10uMATP	12
TEK tyrosine kinase, endothelial _h_wt_AS_10uMATP	12
phosphorylase kinase, gamma 2_h_wt_AS_10uMATP	12
serum/glucocorticoid regulated kinase 1_h_wt_AS_10uMATP	12
interleukin-1 receptor-associated kinase 4_h_wt_AS_10uMATP	12
mitogen-activated protein kinase kinase 1_h_wt_AS_10uMATP	12
phosphoinositide-3-kinase, catalytic, gamma polypeptide_h_wt_AS_10uMATP	12
Janus kinase 3_h_wt_AS_10uMATP	11.5
MAP/microtubule affinity-regulating kinase 2_h_wt_AS_10uMATP	11
p21 protein -activated kinase 2_h_wt_AS_10uMATP	11
Janus kinase 3_h_wt_AS_10uMATP	10.5
EPH receptor A3_h_wt_AS_10uMATP	10
NIMA -related kinase 2_h_wt_AS_10uMATP	10
germ cell associated 2 (haspin)_h_wt_AS_10uMATP	10
protein kinase C, gamma _h_wt_AS_10uMATP	10
glycogen synthase kinase 3 beta_h_wt_AS_10uMATP	10
casein kinase 1, gamma 2 _h_wt_AS_10uMATP	10
LIM domain kinase 1_h_wt_AS_10uMATP	10
EPH receptor A8_h_wt_AS_10uMATP	10
ribosomal protein S6 kinase, 70kDa, polypeptide 1 _h_wt_AS_10uMATP	10
SNF1-like kinase _h_wt_AS_10uMATP	10
v-akt murine thymoma viral oncogene homolog 2 _h_wt_AS_10uMATP	9
muscle, skeletal, receptor tyrosine kinase _h_wt_AS_10uMATP	9
serine/threonine kinase 24 _h_wt_AS_10uMATP	9
ribosomal protein S6 kinase, 90kDa, polypeptide 4_h_wt_AS_10uMATP	9

casein kinase 1, gamma 3_h_wt_AS_10uMATP	9
pim-3 oncogene _h_wt_AS_10uMATP	9
protein kinase C, beta 1_h_wt_AS_10uMATP	9
Janus kinase 3_h_wt_AS_10uMATP	8
EPH receptor B4_h_wt_AS_10uMATP	8
serine/threonine kinase 10_h_wt_AS_10uMATP	8
calcium/calmodulin-dependent protein kinase II delta _h_wt_AS_10uMATP	8
protein kinase, AMP-activated, alpha 1 catalytic subunit_h_wt_AS_10uMATP	8
fms-related tyrosine kinase 1_h_wt_AS_10uMATP	7
myosin light chain kinase_h_wt_AS_10uMATP	7
p21 protein -activated kinase 5_h_wt_AS_10uMATP	7
v-akt murine thymoma viral oncogene homolog 1_h_wt_AS_10uMATP	7
mitogen-activated protein kinase-activated protein kinase 5_h_wt_AS_10uMATP	7
mitogen-activated protein kinase kinase 6_h_wt_AS_10uMATP	7
BR serine/threonine kinase 1_h_wt_AS_10uMATP	6
nemo-like kinase _h_wt_AS_10uMATP	6
eukaryotic elongation factor-2 kinase _h_wt_AS_10uMATP	6
mitogen-activated protein kinase 11_h_wt_AS_10uMATP	6
TYRO3 protein tyrosine kinase_h_wt_AS_10uMATP	6
protein kinase C, epsilon _h_wt_AS_10uMATP	6
mitogen-activated protein kinase 1_h_wt_AS_10uMATP	6
NIMA -related kinase 11_h_wt_AS_10uMATP	6
macrophage stimulating 1 receptor_h_wt_AS_10uMATP	6
CDC-like kinase 2 _h_wt_AS_10uMATP	6
Janus kinase 3_h_wt_AS_10uMATP	5
inhib of kappa light polypeptide gene enhancer in B-cells, kinase beta _h_wt_AS_10uMATP	5
EPH receptor A5_h_wt_AS_10uMATP	5
v-yes-1 Yamaguchi sarcoma viral oncogene homolog 1 _h_wt_AS_10uMATP	5
CHK2 checkpoint homolog (S. pombe)_h_wt_AS_10uMATP	5
casein kinase 1, gamma 1_h_wt_AS_10uMATP	5
casein kinase 1, delta _h_wt_AS_10uMATP	5
platelet-derived growth factor receptor, alpha polypeptide _h_wt_AS_10uMATP	5

v-kit Hardy-Zuckerman 4 feline sarcoma viral oncogene homolog_h_wt_AS_10uMATP	5
TAO kinase 1_h_wt_AS_10uMATP	5
fms-related tyrosine kinase 3_h_wt_AS_10uMATP	4
neurotrophic tyrosine kinase, receptor, type 1_h_wt_AS_10uMATP	4
testis-specific serine kinase 1B _h_wt_AS_10uMATP	4
phosphoinositide-3-kinase, catalytic, delta polypeptide_h_wt_AS_10uMATP	4
calcium/calmodulin-dependent protein kinase II beta _h_wt_AS_10uMATP	4
CDC42 binding protein kinase alpha (DMPK-like) _h_wt_AS_10uMATP	4
EPH receptor A1 _h_wt_AS_10uMATP	3
CHK1 checkpoint homolog (S. pombe)_h_wt_AS_10uMATP	3
v-akt murine thymoma viral oncogene homolog 3 _h_wt_AS_10uMATP	3
protein kinase D1 _h_wt_AS_10uMATP	3
protein kinase C, zeta _h_wt_AS_10uMATP	3
death-associated protein kinase 2_h_wt_AS_10uMATP	3
c-abl oncogene 1, receptor tyrosine kinase _h_wt_AS_10uMATP	3
maternal embryonic leucine zipper kinase _h_wt_AS_10uMATP	3
aurora kinase B_h_wt_AS_10uMATP	3
Janus kinase 3_h_wt_AS_10uMATP	2.5
ribosomal protein S6 kinase, 90kDa, polypeptide 5 _h_wt_AS_10uMATP	2
unc-51-like kinase 3_h_wt_AS_10uMATP	2
pim-2 oncogene _h_wt_AS_10uMATP	2
protein kinase C, alpha _h_wt_AS_10uMATP	2
serum/glucocorticoid regulated kinase family, member 3_h_wt_AS_10uMATP	2
ribosomal protein S6 kinase, 90kDa, polypeptide 3 _h_wt_AS_10uMATP	2
Janus kinase 3_h_wt_AS_10uMATP	1.5
Janus kinase 3_h_wt_AS_10uMATP	1.5
Janus kinase 3_h_wt_AS_10uMATP	1
phosphoinositide-3-kinase, catalytic, beta polypeptide _h_wt_AS_10uMATP	1
mitogen-activated protein kinase-activated protein kinase 3_h_wt_AS_10uMATP	1
homeodomain interacting protein kinase 2_h_mt_AS_10uMATP	1
EPH receptor A7_h_wt_AS_10uMATP	1
serum/glucocorticoid regulated kinase 2_h_wt_AS_10uMATP	1

TAO kinase 2_h_mt_AS_10uMATP	1
mitogen-activated protein kinase kinase kinase kinase 2 _h_wt_AS_10uMATP	1
casein kinase 2, alpha 1 polypeptide _h_wt_AS_10uMATP	1
serine/threonine kinase 3 _h_wt_AS_10uMATP	1
death-associated protein kinase 1_h_wt_AS_10uMATP	1
phosphatidylinositol-4-phosphate 5-kinase, type I, alpha_h_wt_AS_10uMATP	1
phosphoinositide-3-kinase catalytic alpha polypeptide p85_h_wt_AS_10uMATP	1
MAP kinase interacting serine/threonine kinase 2_h_wt_AS_10uMATP	0
serine/threonine kinase 4_h_wt_AS_10uMATP	0
cyclin-dependent kinase 1 / clyclinB_h_wt_AS_10uMATP	0
SFRS protein kinase 1_h_wt_AS_10uMATP	0
tousled-like kinase 2_h_wt_AS_10uMATP	0
PTK2B protein tyrosine kinase 2 beta _h_wt_AS_10uMATP	0
aurora kinase A_h_wt_AS_10uMATP	0
polo-like kinase 1_h_wt_AS_10uMATP	0
unc-51-like kinase 2_h_wt_AS_10uMATP	0
phosphatidylinositol-5-phosphate 4-kinase, type II, alpha _h_wt_AS_10uMATP	0
Janus kinase 3_h_wt_AS_10uMATP	-0.5
protein kinase C, beta 2_h_wt_AS_10uMATP	-1
protein kinase, cGMP-dependent, type II _h_wt_AS_10uMATP	-1
calcium/calmodulin-dependent protein kinase I _h_wt_AS_10uMATP	-1
serine/threonine kinase 11_h_wt_AS_10uMATP_	-1
feline sarcoma oncogene _h_wt_AS_10uMATP	-1
casein kinase 2, alpha prime polypeptide _h_wt_AS_10uMATP	-1
fibroblast growth factor receptor 4_h_wt_AS_10uMATP	-1
pim-1 oncogene _h_wt_AS_10uMATP	-1
insulin-like growth factor 1 receptor _h_wt_AS_10uMATP	-1
platelet-derived growth factor receptor, beta polypeptide _h_wt_AS_10uMATP	-1
doublecortin-like kinase 2_h_wt_AS_10uMATP	-1
conserved helix-loop-helix ubiquitous kinase _h_wt_AS_10uMATP	-1
NIMA -related kinase 3_h_wt_AS_10uMATP	-1
mechanistic target of rapamycin / FKBP12_h_wt_AS_10uMATP	-1
insulin receptor-related receptor_h_wt_AS_10uMATP	-2

AXL receptor tyrosine kinase _h_wt_AS_10uMATP	-2
G protein-coupled receptor kinase 6_h_wt_AS_10uMATP	-2
polo-like kinase 3_h_wt_AS_10uMATP	-2
G protein-coupled receptor kinase 5_h_wt_AS_10uMATP	-2
dual-specificity tyrosine-(Y)-phosphorylation regulated kinase 2 _h_wt_AS_10uMATP	-2
polo-like kinase 2_h_wt_AS_10uMATP	-2
mitogen-activated protein kinase 12_h_wt_AS_10uMATP	-2
phosphatidylinositol-4-phosphate 5-kinase, type I, gamma_h_wt_AS_10uMATP	-2
zeta-chain associated protein kinase 70kDa_h_wt_AS_10uMATP	-3
cyclin-dependent kinase 3 / cyclinE_h_wt_AS_10uMATP	-3
calcium/calmodulin-dependent protein kinase ID _h_wt_AS_10uMATP	-3
homeodomain interacting protein kinase 1_h_wt_AS_10uMATP	-3
NUAK family, SNF1-like kinase, 1_h_wt_AS_10uMATP	-3
p21 protein -activated kinase 4_h_wt_AS_10uMATP	-3
mitogen-activated protein kinase 14_h_wt_AS_10uMATP	-3
discoidin domain receptor tyrosine kinase 2_h_wt_AS_10uMATP	-3
protein kinase, X-linked _h_wt_AS_10uMATP	-3
G protein-coupled receptor kinase 7_h_wt_AS_10uMATP	-3
ribosomal protein S6 kinase, 90kDa, polypeptide 1 _h_wt_AS_10uMATP	-4
fer (fps/fes related) tyrosine kinase _h_wt_AS_10uMATP	-4
activin A receptor, type 1B_h_wt_AS_10uMATP	-4
3-phosphoinositide dependent protein kinase-1_h_wt_AS_10uMATP	-4
MAP/microtubule affinity-regulating kinase 1_h_wt_AS_10uMATP	-4
colony stimulating factor 1 receptor_h_wt_AS_10uMATP	-4
glycogen synthase kinase 3 alpha_h_wt_AS_10uMATP	-4
mitogen-activated protein kinase 8_h_wt_AS_10uMATP	-4
cyclin-dependent kinase 2 / clyclinA_h_wt_AS_10uMATP	-4
mechanistic target of rapamycin _h_wt_AS_10uMATP	-4
cyclin-dependent kinase 6 / cyclinD3_h_wt_AS_10uMATP	-5
mitogen-activated protein kinase kinase kinase 9_h_wt_AS_10uMATP	-5
SFRS protein kinase 2_h_wt_AS_10uMATP	-5
testis-specific serine kinase 2 _h_wt_AS_10uMATP	-5
CDC-like kinase 3_h_wt_AS_10uMATP	-6
fibroblast growth factor receptor 2_h_wt_AS_10uMATP	-6

NIMA -related kinase 6_h_wt_AS_10uMATP	-6
c-ros oncogene 1 , receptor tyrosine kinase _h_wt_AS_10uMATP	-6
Rho-associated, coiled-coil containing protein kinase 1_h_wt_AS_10uMATP	-6
mitogen-activated protein kinase-activated protein kinase 2_h_wt_AS_10uMATP	-6
vaccinia related kinase 2 _h_wt_AS_10uMATP	-6
cyclin-dependent kinase 9 / cyclinT1_h_wt_AS_10uMATP	-6
calcium/calmodulin-dependent protein kinase II gamma_h_wt_AS_10uMATP	-6
phosphoinositide-3-kinase, class 2, alpha polypeptide _h_wt_AS_10uMATP	-6
protein kinase D2 _h_wt_AS_10uMATP	-7
insulin receptor _h_wt_AS_10uMATP	-7
fibroblast growth factor receptor 3_h_wt_AS_10uMATP	-7
phosphoinositide-3-kinase, class 2, gamma polypeptide _h_wt_AS_10uMATP	-7
cyclin-dependent kinase 2 /clyclinE_h_wt_AS_10uMATP	-8
mitogen-activated protein kinase 9_h_wt_AS_10uMATP	-8
mitogen-activated protein kinase kinase kinase 5_h_wt_AS_10uMATP	-8
TANK-binding kinase 1_h_wt_AS_10uMATP	-8
Rho-associated, coiled-coil containing protein kinase 2_h_wt_AS_10uMATP	-8
homeodomain interacting protein kinase 3_h_wt_AS_10uMATP	-8
NIMA -related kinase 7_h_wt_AS_10uMATP	-8
c-mer proto-oncogene tyrosine kinase_h_wt_AS_10uMATP	-8
IL2-inducible T-cell kinase_h_wt_AS_10uMATP	-8
protein kinase C, delta _h_wt_AS_10uMATP	-8
protein kinase, AMP-activated, alpha 2 catalytic subunit_h_wt_AS_10uMATP	-8
mitogen-activated protein kinase kinase 7_h_wt_AS_10uMATP	-9
p21 protein -activated kinase 6_h_wt_AS_10uMATP	-9
BR serine/threonine kinase 2_h_wt_AS_10uMATP	-9
protein kinase N2 _h_wt_AS_10uMATP	-9
CDC42 binding protein kinase beta (DMPK-like) _h_wt_AS_10uMATP	-9
ribosomal protein S6 kinase, 90kDa, polypeptide 6 _h_wt_AS_10uMATP	-10
mitogen-activated protein kinase 10_h_wt_AS_10uMATP	-10
protein kinase C, iota _h_wt_AS_10uMATP	-10
misshapen-like kinase 1 _h_wt_AS_10uMATP	-10

mitogen-activated protein kinase 13_h_wt_AS_10uMATP	-11
insulin receptor (activated)_h_wt_AS_10uMATP	-11
TAO kinase 3_h_wt_AS_10uMATP	-12
EPH receptor A4_h_wt_AS_10uMATP	-12
cyclin-dependent kinase 5 / p25_h_wt_AS_10uMATP	-12
EPH receptor B3_h_wt_AS_10uMATP	-12
EPH receptor B1 _h_wt_AS_10uMATP	-13
death-associated protein kinase 3_h_wt_AS_10uMATP	-13
cyclin-dependent kinase 5 / p35_h_wt_AS_10uMATP	-13
protein kinase, cGMP-dependent, type I_h_wt_AS_10uMATP	-14
PTK2 protein tyrosine kinase 2_h_wt_AS_10uMATP	-14
mitogen-activated protein kinase 1 (MAPK2)_h_wt_AS_10uMATP	-14
WNK lysine deficient protein kinase 2 _h_wt_AS_10uMATP	-14
calcium/calmodulin-dependent protein kinase IV _h_wt_AS_10uMATP	-14
insulin-like growth factor 1 receptor (activated)_h_wt_AS_10uMATP	-14
fibroblast growth factor receptor 1_h_wt_AS_10uMATP	-15
protein kinase C, theta _h_wt_AS_10uMATP	-15
WNK lysine deficient protein kinase 3_h_wt_AS_10uMATP	-17
ret proto-oncogene _h_wt_AS_10uMATP	-18
protein kinase, cAMP-dependent, catalytic, alpha _h_wt_AS_10uMATP	-19
mitogen-activated protein kinase kinase kinase 7 _h_wt_AS_10uMATP	-19
met proto-oncogene_h_wt_AS_10uMATP	-22
transforming growth factor, beta receptor 1_h_wt_AS_10uMATP	-23
protein kinase C, eta _h_wt_AS_10uMATP	-24
neurotrophic tyrosine kinase, receptor, type 2_h_wt_AS_10uMATP	-25
Janus kinase 2_h_wt_AS_10uMATP	-25
anaplastic lymphoma receptor tyrosine kinase _h_wt_AS_10uMATP	-31

Representative synthesis methods for compounds 9-30

Experimental Details. No unexpected or unusually high safety hazards were encountered. All solvents and chemicals were used as purchased without further purification. Nuclear magnetic resonance (NMR) spectra were obtained on Bruker model DRX spectrometers. Chemical shifts (δ) are expressed in parts per million, relative to internal tetramethylsilane; coupling constants (J) are in hertz (Hz). The following abbreviations are used to describe peak patterns when appropriate: s (singlet), d (doublet), t (triplet), q (quartet), qt (quintet), m (multiplet), app (apparent), and br (broad). HPLC−MS chromatograms and spectra were obtained using one of the following methods, and purity of all final compounds was confirmed to be >95%: (1) Agilent 1200 HPLC and G6100 system on X-Bridge ShieldRP18 (50 × 2.1 mm, 5 μm) and a gradient system of 0.05% NH_4OH in H_2O/CH_3CN, 100:0 to 5:95 over 7.5 min, then 100:0 for 2.5 min at a temperature of 40 °C; (2) Agilent 1200 HPLC and G6100 system on Phenomenex Luna-C18 (50 × 2 mm, 5 μm) and a gradient system of 0.1% TFA in H_2O/0.05% TFA in CH_3CN, 100:0 to 15:85 over 7.5 min, then 100:0 for 2.5 min at a temperature of 50 °C; or (3) Agilent 1100 HPLC and G1367A system on X-Bridge C18 (100 × 3 mm, 3.5uM) and a gradient system of 20 mM NH_4OH in H_2O/CH_3CN 90:10 over 2 min, then 0:100 for 1 min at a flow rate of 2.4 mL/min at a temperature of 45 °C. All compounds tested were of a minimum of 95% purity as determined by HPLC.

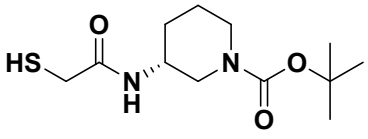

tert-Butyl (3*R*)-3-[(2-sulfanylacetyl)amino]piperidine-1-carboxylate. To a 10-20 mL microwave vial was added (*R*)-1-boc-3-aminopiperidine (5.02 g, 25.0 mmol). The vial was sealed and evacuated and back-filled with argon three times and then methyl 2-mercaptoacetate (6.7 mL, 75 mmol) was added via syringe in one portion and the vial was heated in a 150 °C oil bath. After 1

h 35 minutes, the mixture was cooled to room temperature and was purified by FCC (SiO_2, EtOAc/hexanes) to give the title compound (5.54 g, 80.6%). The purified product contained the disulfide (di-*tert*-butyl 3,3'-((2,2'-disulfanediylbis(acetyl))bis(azanediyl))(3*R*,3'*R*)-bis(piperidine-1-carboxylate)) as a biproduct, but was used as is in the next reaction. MS (ESI): mass calcd. for $C_8H_{15}N_2O_3S$, 219.08 $[M\text{-}tBu+H]^+$; m/z found, 219.1. ^1H NMR (400 MHz, $CDCl_3$): δ 6.73-7.00 (br m, 1H), 3.96 (br s, 1H), 3.14-3.66 (m, 6H), 1.53-1.91 (m, 5H), 1.47 (s, 9H).

General method 1: Compound 10.

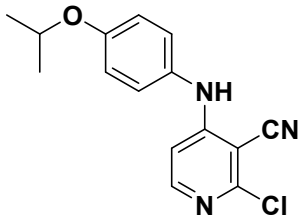

2-Chloro-4-(4-isopropoxyanilino)pyridine-3-carbonitrile. To a 20 mL microwave vial was added sequentially 2-chloro-4-iodonicotinonitrile (300 mg, 1.13 mmol), 4-isopropoxyaniline (172 mg, 1.13 mmol), palladium(II) acetate (5.0 mg, 0.023 mmol), bis(2-diphenylphosphinophenyl)ether (18 mg, 0.034 mmol), and Cs_2CO_3 (517 mg, 1.59 mmol) and the vial was sealed and evacuated and refilled with argon three times. To this vial was added 1,4-dioxane (2.2 mL) and the vial was evacuated and refilled with argon once. The reaction mixture was heated for 5 minutes in a 50 °C oil bath under an argon inlet needle, then the inlet needle was removed, and the sealed vial was heated for 30 minutes in a 150 °C oil bath. The crude reaction mixture was used directly in the next step. MS (ESI): mass calcd. for $C_{15}H_{15}ClN_3O$ $[M+H]^+$ 288.01; m/z found, 288.3.

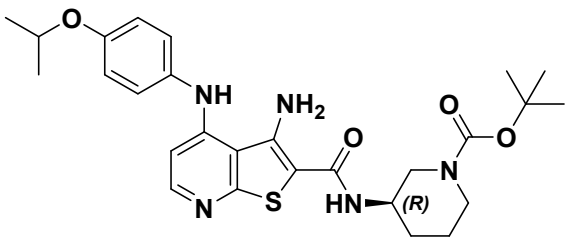

(*R*)-*tert*-Butyl 3-(3-amino-4-((4-isopropoxyphenyl)amino)thieno[2,3-*b*]pyridine-2-carboxamido)piperidine-1-carboxylate. To the sealed tube containing 2-chloro-4-(4-isopropoxyanilino)pyridine-3-carbonitrile (326 mg, 1.13 mmol) was added a solution of *tert*-butyl (3*R*)-3-[(2-sulfanylacetyl)amino]piperidine-1-carboxylate in dioxane (0.5 M, 2.7 mL, 1.4 mmol). The resulting brown suspension was heated in the sealed tube in a 150 °C oil bath for 15 minutes. The mixture was cooled to room temperature to give the title compound as a crude mixture, which was used in the next reaction without purification. MS (ESI): mass calcd. for $C_{27}H_{36}N_5O_4S$, 526.25 $[M+H]^+$; m/z found, 526.5.

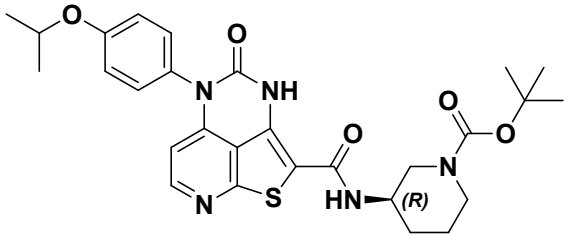

(*R*)-*tert*-Butyl 3-(5-(4-isopropoxyphenyl)-4-oxo-4,5-dihydro-3*H*-1-thia-3,5,8-triazaacenaphthylene-2-carboxamido)piperidine-1-carboxylate. To the crude mixture of (*R*)-*tert*-butyl 3-(3-amino-4-((4-isopropoxyphenyl)amino)thieno[2,3-*b*]pyridine-2-carboxamido)piperidine-1-carboxylate was added 1,1´-carbonyldiimidazole (0.736 g, 4.54 mmol). The tube was sealed, and the vessel was evacuated and refilled with argon twice. The mixture was heated for 5 minutes in a 50 °C oil bath under an argon inlet needle, then the argon inlet needle was removed, and the mixture was heated at 150 °C for 10 minutes. The mixture was cooled to room temperature and was partitioned between EtOAc (50 mL) and H_2O (50 mL). The aqueous phase was extracted with EtOAc (2 x 50 mL) and the combined organic extracts were washed with saturated aqueous NaCl (50 mL), followed by 1 N aqueous HCl (50 mL). The organic phase was dried over anhydrous Na_2SO_4, filtered, and concentrated to dryness. The residue was purified FCC (SiO_2, EtOAc/hexanes) to give the title compound as a tan foamy solid (449 mg, 72%). MS (ESI):

mass calcd. for $C_{28}H_{34}N_5O_5S$, 552.23; m/z found, 552.5 $[M+H]^+$. ^1H NMR (400 MHz, $CDCl_3$): δ 9.47 (s, 1H), 8.34 (d, *J*=5.56 Hz, 1H), 7.19-7.25 (m, 2H), 7.04 (d, *J*=9.09 Hz, 2H), 6.13 (d, *J*=5.56 Hz, 1H), 4.60 (spt, *J*=6.06 Hz, 1H), 4.08-4.16 (m, 1H), 3.23-3.68 (m, 4H), 1.66-1.96 (m, 3H), 1.50 (s, 9H), 1.43-1.47 (m, 1H), 1.39 (d, *J*=6.06 Hz, 6H).

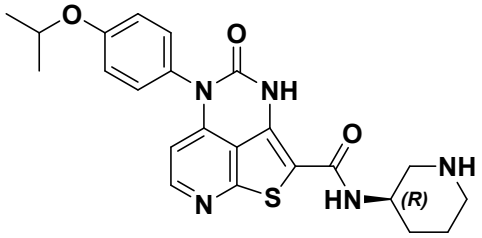

Compound 9: (*R*)-5-(4-Isopropoxyphenyl)-4-oxo-*N*-(piperidin-3-yl)-4,5-dihydro-3*H*-1-thia-3,5,8-triazaacenaphthylene-2-carboxamide hydrochloride. To a solution of (*R*)-*tert*-butyl 3-(5-(4-isopropoxyphenyl)-4-oxo-4,5-dihydro-3*H*-1-thia-3,5,8-triazaacenaphthylene-2-carboxamido)piperidine-1-carboxylate (421.8 mg, 0.765 mmol) in dioxane (4 mL) was added HCl in dioxane (4.0 mL, 4.0 M, 16 mmol) and the mixture was stirred at room temperature under air for 20 minutes. The reaction mixture was concentrated to dryness and the residue was dried under vacuum to give the crude title compound as a tan powder (459.2 mg, crude). MS (ESI): mass calcd. for $C_{23}H_{26}N_5O_3S$, 452.18 $[M+H]^+$; m/z found, 452.1. ^1H NMR (400 MHz, DMSO-d_6): δ 10.17 (s, 1H), 8.62-8.80 (m, 2H), 8.38 (d, *J* = 5.56 Hz, 1H), 8.21 (d, *J* = 7.07 Hz, 1H), 7.38 (d, *J* = 7.58 Hz, 2H), 7.15 (d, *J* = 9.09 Hz, 2H), 6.09 (d, *J* = 5.56 Hz, 1H), 4.74 (spt, *J* = 5.89 Hz, 1H), 4.14-4.26 (m, 1H), 3.24-3.43 (m, 2H), 2.80–2.95 (m, 2H), 1.88-2.02 (m, 2H), 1.60-1.82 (m, 2H), 1.37 (d, 6H).

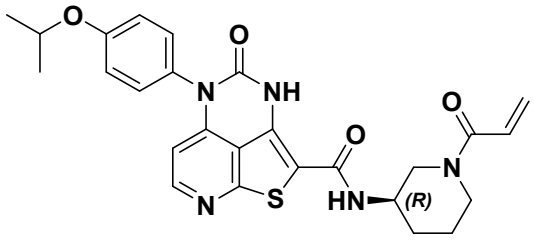

Compound 10: (*R*)-*N*-(1-Acryloylpiperidin-3-yl)-5-(4-isopropoxyphenyl)-4-oxo-4,5-dihydro-3*H*-1-thia-3,5,8-triazaacenaphthylene-2-carboxamide. To a solution of (*R*)-5-(4-isopropoxyphenyl)-4-oxo-*N*-(piperidin-3-yl)-4,5-dihydro-3*H*-1-thia-3,5,8-triazaacenaphthylene-2-carboxamide•HCl (93.2 mg, 0.191 mmol) in DCM (1 mL) was added TEA (79 µL, 0.57 mmol) followed by acryloyl

chloride (15 µL, 0.19 mmol) dropwise via syringe. The resulting suspension was stirred under air at 0 °C for 40 min. The reaction mixture was partitioned between DCM (10 mL) and saturated aqueous $NaHCO_3$ (10 mL). The aqueous phase was extracted once with EtOAc (10 mL) and the combined organic extracts were dried over anhydrous Na_2SO_4, filtered, and concentrated to dryness. The residue was purified by FCC (SiO_2, EtOAc/hexanes) to give the title compound as a yellow powder (32.2 mg, 33%). MS (ESI): mass calcd. for $C_{26}H_{28}N_5O_4S$, 506.19 $[M+H]^+$; m/z found, 506.2. ^1H NMR (400 MHz, $CDCl_3$): δ 9.46 (s, 1H), 8.34 (br s., 1H), 7.22 (d, *J* = 7.58 Hz, 2H), 7.04 (d, *J* = 8.59 Hz, 2H), 6.63 (dd, *J* = 10.86, 16.93 Hz, 1H), 6.28-6.49 (m, 1H), 6.24 (br. s., 0.5H), 6.06-6.19 (m, 1H), 5.68-5.82 (m, 1H), 5.49 (br. s., 0.5H), 4.60 (spt, *J* = 5.98 Hz, 1H), 3.84-4.24 (m, 2.5H), 3.28-3.77 (m, 2.5H), 1.68-2.14 (m, 4H), 1.39 (d, *J* = 6.06 Hz, 6H).

General Method 2: Compound 16

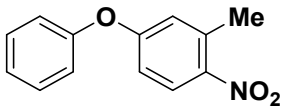

Compound 32: 2-Methyl-1-nitro-4-phenoxybenzene. To a round bottom flask were added phenol (42.5 g, 452 mmol), K_2CO_3 (125 g, 905 mmol), and DMF (500 mL). To the reaction mixture was added 5-fluoro-2-nitrotoluene (70.2 g, 452 mmol) and the reaction was stirred at 80 °C for 16 h under N_2. The reaction was diluted with saturated NH_4Cl and extracted with MTBE (3 3 400 mL). The organic layers were combined, dried over anhydrous Na_2SO_4, filtered, and concentrated to dryness to yield the title compound (100 g, 92% yield) as a brown oil.

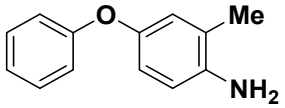

Compound 33: 2-Methyl-4-phenoxyaniline. To a solution of 2-methyl-1-nitro-4-phenoxybenzene (100 g, 436 mmol) in EtOH/H_2O (3:1 ratio, 2000 mL) were sequentially added NH_4Cl (117 g, 2180 mmol) and Fe (97 g, 1700 mmol). The reaction mixture was heated to reflux for 2 h, then the reaction was cooled to 25 °C and concentrated to dryness. To the residue was added water and EtOAc and the organic layer was separated, washed with saturated $NaHCO_3$ and saturated brine, dried over anhydrous MgSO4, filtered, and concentrated to dryness to yield the title compound (82 g, 90% yield).

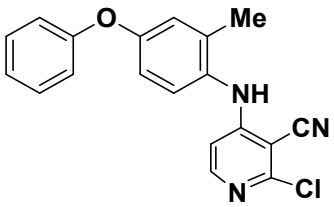

Compound 34: 2-Chloro-4-(2-methyl-4-phenoxyanilino)pyridine-3-carbonitrile. To a round bottom flask under a N_2 atmosphere were added 2-methyl-4-phenoxyaniline (30 g, 150 mmol), 2-chloro-4-iodopyridine-3-carbonitrile (51.6 g, 195 mmol), and dioxane (200 mL), followed by bis(2-diphenylphosphinophenyl)ether (16 g, 30 mmol), $Pd(OAc)_2$ (3.36 g, 15 mmol), and K_3PO_4 (89 g, 420 mmol). The reaction mixture was stirred at 100 °C overnight. The reaction mixture was filtered and purified FCC (SiO_2, EtOAc/hexanes)to yield the title compound as a yellow solid (32 g, 63% yield). MS (ESI): mass calcd. for $C_{19}H_{15}ClN_3O$, 336.09 $[M+H]^+$; m/z found, 336.0.

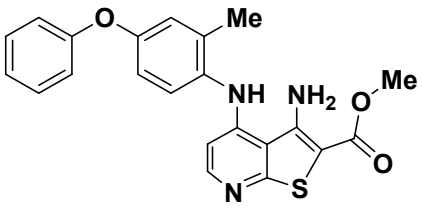

Compound 35: Methyl 3-amino-4-(2-methyl-4-phenoxyanilino)thieno[2,3-*b*]pyridine-2-carboxylate. To a round bottom flask were added 2-chloro-4-(2-methyl-4-phenoxyanilino)pyridine-3-carbonitrile (36 g, 107 mmol) in MeOH (150 mL). To this solution was added NaOMe (14.5 g, 268 mmol) in MeOH (30 mL), followed by methyl 2-sulfanylacetate (23 g, 217 mmol). The reaction mixture was refluxed overnight. The reaction mixture was cooled, and the yellow precipitate was isolated by filtration, washed with MeOH, and dried to yield the title compound as a yellow solid (30 g, 75% yield). MS (ESI): mass calcd. for $C_{22}H_{20}N_3O_3S$ $[M+H]^+$ 406.12; m/z found, 406.1.

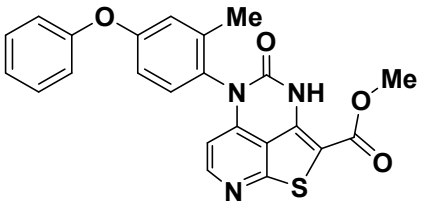

Compound 36: Methyl 5-(2-methyl-4-phenoxyphenyl)-4-oxo-4,5-dihydro-3*H*-1-thia-3,5,8-triazaacenaphthylene-2-carboxylate. To a round bottom flask were added methyl 3-amino-4-(2-

methyl-4-phenoxyanilino)thieno[2,3-*b*]pyridine-2-carboxylate (30.6 g, 75.5 mmol), carbonyl diimidazole (49.0 g, 300 mmol), and 1,4-dioxane (500 ml). The reaction was stirred at reflux overnight. Then the reaction mixture was concentrated to dryness and to the residue was added to MeOH (200 mL) and the precipitate that formed was filtered off and dried to yield the title compound as a yellow solid (28.1 g, 86% yield). MS (ESI): mass calcd. for $C_{23}H_{18}N_3O_4S$, 432.10 $[M+H]^+$; m/z found, 432.1.

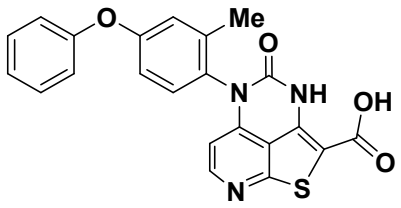

Compound 37: 5-(2-Methyl-4-phenoxyphenyl)-4-oxo-4,5-dihydro-3*H*-1-thia-3,5,8-triazaacenaphthylene-2-carboxylic acid. To a round bottom flask were added methyl 5-(2-methyl-4-phenoxyphenyl)-4-oxo-4,5-dihydro-3*H*-1-thia-3,5,8-triazaacenaphthylene-2-carboxylate (9.2 g, 21 mmol), lithium hydroxide (4.47 g, 106 mmol), THF (200 mL), MeOH (200 mL), and H_2O (50 mL). The reaction mixture was stirred at 50 °C for 15 h. The mixture was concentrated to dryness and diluted with H_2O. The pH was adjusted to 2 with 1 M aqueous HCl and the precipitate was filtered and dried to yield the title compound as yellow solid (8.10 g, 91% yield). MS (ESI): mass calcd. for $C_{22}H_{16}N_3O_4S$, 418.09 $[M+H]^+$; m/z found, 418.2.

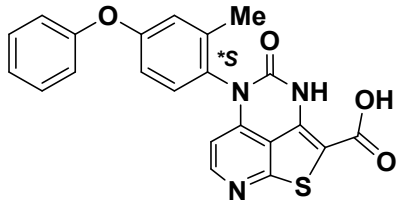

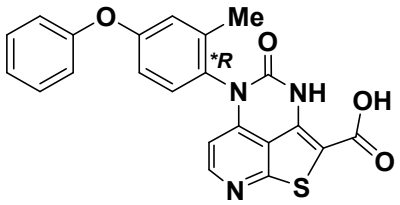

Compounds 38a and 38b: 5-(**S*)-(2-Methyl-4-phenoxyphenyl)-4-oxo-4,5-dihydro-3*H*-1-thia-3,5,8-triazaacenaphthylene-2-carboxylic acid. 5-(2-Methyl-4-phenoxyphenyl)-4-oxo-4,5-dihydro-3*H*-1-thia-3,5,8-triazaacenaphthylene-2-carboxylic acid, as a mixture of atropisomers, was Was resolved on a chiral SFC column (Stationary phase: Whelk O1 (*S*,*S*), 5 µm, 250 × 21.1mm column. The mobile phase was: 40% CO_2, 60% MeOH (0.2% formic acid). The first eluting atropisomer arbitrarily labeled **R* and the second as *S, to indicate that the compound is a single

atropisomer of unknown absolute configuration. MS (ESI): mass calcd. for $C_{22}H_{16}N_3O_4S$ $[M+H]^+$, 418.09; m/z found, 418.2.

Compound 16: (*R*)-*N*-(1-Acryloylpiperidin-3-yl)-5-(**R*)-(2-methyl-4-phenoxyphenyl)-4-oxo-4,5-dihydro-3*H*-1-thia-3,5,8-triazaacenaphthylene-2-carboxamide.

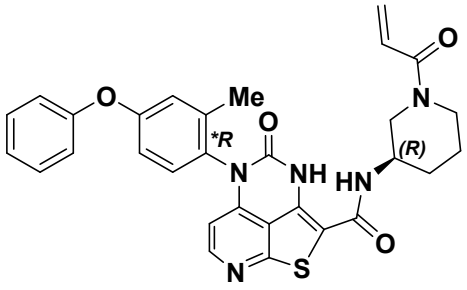

To a round bottom flask were added 5-(**R*)-(2-methyl-4-phenoxyphenyl)-4-oxo-4,5-dihydro-3*H*-1-thia-3,5,8-triazaacenaphthylene-2-carboxylic acid (100 mg, 0.24 mmol), DMF (3 mL), HATU (183 mg, 0.481 mmol), and TEA (73 mg, 0.72 mmol) and allowed to stir for 10 min. (*R*)-1-(3-aminopiperidin-1-yl)prop-2-en-1-one (55 mg, 0.29 mmol) was added and the mixture was stirred for 2 hours. The crude mixture was purified by HPLC ($MeOH/H_2O$) to provide the desired compound as a slight yellow solid (30 mg, 32%). MS (ESI): mass calcd. for $C_{30}H_{28}N_5O_4S$, 554.19 $[M+H]^+$; m/z found, 554.0. ^1H NMR (400 MHz, DMSO-d_6): δ 10.29-10.20 (m, 1H), 8.37-8.32 (m, 1H), 8.13-8.04 (m, 1H), 7.50-7.35 (m, 3H), 7.25-7.17 (m, 1H), 7.17-7.07 (m, 3H), 7.02-6.95 (m, 1H), 6.87-6.73 (m, 1H), 6.16-6.06 (m, 1H), 6.03-5.97 (m, 1H), 5.72-5.64 (m, 1H), 4.54-4.18 (m, 1H), 4.10-3.95 (m, 1H), 3.84-3.74 (m, 1H), 3.17-2.92 (m, 1H), 2.82-2.62 (m, 1H), 2.07 (s, 3H), 2.00-1.88 (m, 1H), 1.84-1.74 (m, 1H), 1.74-1.61 (m, 1H), 1.51-1.36 (m, 1H).

General method 3: Compound 28

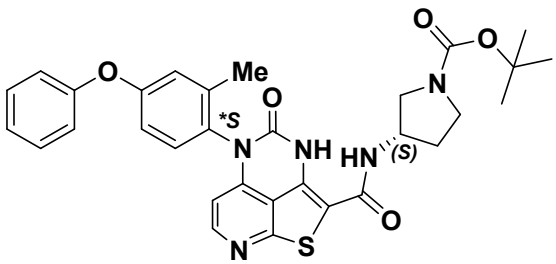

tert-Butyl (*S*)-3-(5-(**S*)-(2-methyl-4-phenoxyphenyl)-4-oxo-4,5-dihydro-3*H*-1-thia-3,5,8-triazaacenaphthylene-2-carboxamido)pyrrolidine-1-carboxylate. To a stirred suspension of 5-(**S*)-(2-methyl-4-phenoxyphenyl)-4-oxo-4,5-dihydro-3*H*-1-thia-3,5,8-triazaacenaphthylene-2-carboxylic acid (120 mg, 0.287 mmol) was added *tert*-butyl (*S*)-3-aminopyrrolidine-1-carboxylate (107 mg, 0.574 mmol), HATU (142 mg, 0.373 mmol), DIEA (55.3 μL, 0.574 mmol), and DMF (5 mL). The resulting mixture was stirred for 1 h at room temperature. The solvent was removed, and the residue was partitioned between EtOAc and H_2O. The crude reaction mixture was by HPLC (MeOH/H_2O), yielding the title compound as a yellow solid (128 mg, 76%). MS (ESI): mass calcd. for $C_{31}H_{32}N_5O_5S$, 586.21 $[M+H]^+$; m/z found, 586.3.

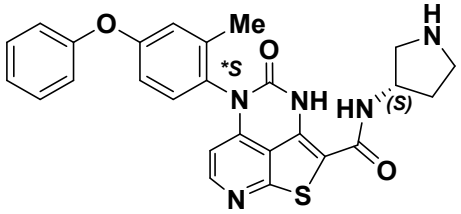

(*S*)-5-(**S*)(2-Methyl-4-phenoxyphenyl)-4-oxo-*N*-(pyrrolidin-3-yl)-4,5-dihydro-3*H*-1-thia-3,5,8-triazaacenaphthylene-2-carboxamide. t*ert*-Butyl (*S*)-3-(5-(**S*)(2-methyl-4-phenoxyphenyl)-4-oxo-4,5-dihydro-3*H*-1-thia-3,5,8-triazaacenaphthylene-2-carboxamido)pyrrolidine-1-carboxylate (128 mg, 0.219 mmol) in MeOH (3 mL) was treated with a solution of concentrated aqueous HCl (12 M, 3 mL). The mixture was stirred at room temperature for 1 h. The solvent was evaporated, and the residue was purified by HPLC to afford the title compound as a yellow solid (111 mg, 100%). MS (ESI): mass calcd. for $C_{26}H_{24}N_5O_3S$ $[M+H]^+$, 486.16; m/z found, 486.3.

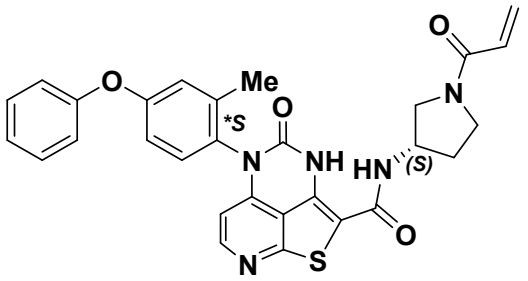

Compound 28: (*S*)-*N*-(1-Acryloylpyrrolidin-3-yl)-5-(**S*)-(2-methyl-4-phenoxyphenyl)-4-oxo-4,5-dihydro-3*H*-1-thia-3,5,8-triazaacenaphthylene-2-carboxamide. To a solution of (*S*)-5(**S*)-(2-methyl-4-phenoxyphenyl)-4-oxo-*N*-(pyrrolidin-3-yl)-4,5-dihydro-3*H*-1-thia-3,5,8-triazaacenaphthylene-2-carboxamide (111 mg, 0.229 mmol) in DCM (10 ml) at 0 °C was added DIPEA (59.1 mg, 0.458 mmol), followed by acryloyl chloride (19 mg, 0.21 mmol). The reaction mixture was removed from the cooling bath and stirred for 1 h. The mixture concentrated then purified by FCC (SiO_2, MeOH/DCM) to afford the title compound (55 mg, 44%) as a white solid. MS (ESI): mass calcd. for $C_{29}H_{26}N_5O_4S$, 540.17 $[M+H]^+$; m/z found, 540.5. ^1H NMR (400 MHz, a mixture of DMSO-d_6 and CD_3OD): δ 8.32-8.24 (m, 1H), 7.42-7.35 (m, 2H), 7.35-7.30 (m, 1H), 7.18-7.11 (m, 1H), 7.10-7.01 (m, 3H), 6.97-6.90 (m, 1H), 6.62-6.48 (m, 1H), 6.21-6.11 (m, 1H), 6.00-5.94 (m, 1H), 5.70-5.61 (m, 1H), 4.58-4.44 (m, 1H), 3.75-3.67 (m, 1H), 3.64-3.57 (m, 1H), 3.56-3.39 (m, 2H), 2.26-2.08 (m, 1H), 2.05 (s, 3H), 2.03-1.95 (m, 1H).

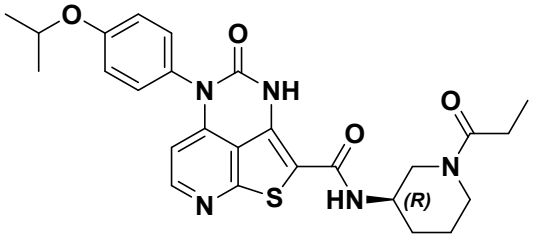

Compound 11: (*R*)-5-(4-Isopropoxyphenyl)-4-oxo-*N*-(1-propionylpiperidin-3-yl)-4,5-dihydro-3*H*-1-thia-3,5,8-triazaacenaphthylene-2-carboxamide. To a solution of (*R*)-5-(4-isopropoxyphenyl)-4-oxo-*N*-(piperidin-3-yl)-4,5-dihydro-3*H*-1-thia-3,5,8-triazaacenaphthylene-2-carboxamide hydrochloride (88.8 mg, 0.182 mmol) in DCM (1 mL) was added TEA (76 µL, 0.55 mmol). The resulting solution was cooled in an ice bath and propionyl chloride (16 µL, 0.18 mmol) was added dropwise via a microliter syringe and the resulting orange solution was stirred

under air in the ice bath for 25 min. The reaction mixture was partitioned between DCM (10 mL) and saturated aqueous $NaHCO_3$ (10 mL). The aqueous phase was extracted once with EtOAc (10 mL) and the combined organic extracts were dried over anhydrous Na_2SO_4, filtered, and concentrated to dryness. The residue was purified by FCC (SiO_2, EtOAc/hexanes) to give the title compound as a light-yellow powder (41.5 mg, 45%). MS (ESI): mass calcd. for $C_{26}H_{30}N_5O_4S$, 508.20 $[M+H]^+$; m/z found, 508.3. ^1H NMR (400 MHz, DMSO-d_6, 1:1 mixture of rotamers): δ 10.18 (s, 0.5H), 10.12 (s, 0.5H), 8.33 (d, J = 5.56 Hz, 1H), 8.10 (d, J = 7.07 Hz, 0.5H), 8.02 (d, J = 7.58 Hz, 0.5H), 7.34 (d, J = 9.09 Hz, 2H), 7.10 (d, J = 9.09 Hz, 2H), 6.01 – 6.05 (m, 1H), 4.70 (spt, J = 5.98 Hz, 1H), 4.33-4.50 (m, 0.5H), 4.19–4.27 (m, 0.5H), 3.70-3.95 (m, 2H), 2.86-3.02 (m, 1H), 2.53-2.68 (m, 1H), 2.30-2.38 (m, 2H), 1.87–1.97 (m, 1H), 1.35-1.80 (m, 3H), 1.33 (d, J = 6.06 Hz, 6H), 1.01 (q, J = 7.07 Hz, 3H).

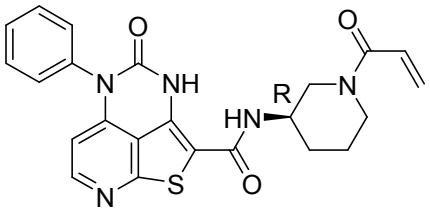

Compound 12: (*R*)-N-(1-acryloylpiperidin-3-yl)-4-oxo-5-phenyl-4,5-dihydro-3H-1-thia-3,5,8-triazaacenaphthylene-2-carboxamide. Compound 12 was prepared using general method 3. MS (ESI): mass calcd. for $C_{23}H_{22}N_5O_3S$, 448.14 $[M+H]^+$; m/z found, 447.9. ^1H NMR (400 MHz, DMSO-d_6): δ 10.20 (d, J = 14.4 Hz, 1H), 8.33 (d, J = 5.5 Hz, 1H), 8.16-8.04 (m, 1H), 7.64-7.60 (m, 2H), 7.57-7.54 (m, 1H), 7.48 (d, J = 7.1 Hz, 2H), 6.87-6.75 (m, 1H), 6.12 (d, J = 16.7 Hz, 1H), 5.99 (d, J = 5.5 Hz, 1H), 5.70 (d, J = 10.7 Hz, 1H), 4.50-4.21 (m, 1H), 4.08-3.99 (m, 1H), 3.79 (s, 1H), 3.17-2.94 (m, 1H), 2.77-2.64 (m, 1H), 1.97-1.94 (m, 1H), 1.81-1.78 (m, 1H), 1.74-1.57 (m, 1H), 1.43 (brs, 1H).

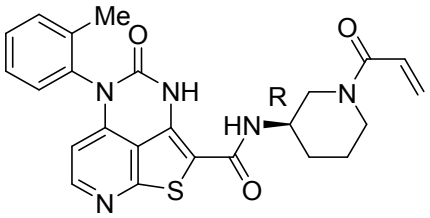

Compound 13: (*R*)-*N*-(1-Acryloylpiperidin-3-yl)-4-oxo-5-(o-tolyl)-4,5-dihydro-3*H*-1-thia-3,5,8-triazaacenaphthylene-2-carboxamide. Compound 13 was prepared using general method 3. MS (ESI): mass calcd. for $C_{24}H_{24}N_5O_3S$, 462.16 $[M+H]^+$; m/z found, 462.1. ^1H NMR (400 MHz, CD_3OD): δ 8.29 (d, *J* = 5.5, 1H), 7.48-7.39 (m, 3H), 7.35-7.30 (m, 1H), 6.86-6.71 (m, 1H), 6.25-6.14 (m, 1H), 5.96 (d, *J* = 5.5, 1H), 5.76-5.67 (m, 1H), 4.56-4.26 (m, 1H), 4.21-3.90 (m, 2H), 3.20-3.11 (m, 1H), 2.65-2.82 (m, 1H), 2.16 (s, 3H), 2.09-2.01 (m, 1H), 1.90-1.82 (m, 1H), 1.80-1.22 (m, 1H), 1.63-1.52 (m, 1H).

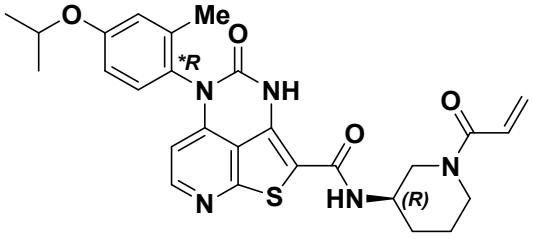

Compound 14, Step G: (*R*)-*N*-(1-Acryloylpiperidin-3-yl)-5-(**R*)-(4-isopropoxy-2-methylphenyl)-4-oxo-4,5-dihydro-3*H*-1-thia-3,5,8-triazaacenaphthylene-2-carboxamide. Compound 13 was prepared using general method 3. MS (ESI): mass calcd. for $C_{27}H_{30}N_5O_4S$, 520.20 $[M+H]^+$; m/z found, 520.2. ^1H NMR (400 MHz, CD_3OD): δ 8.31 (d, *J* = 5.56 Hz, 1H), 7.21 (d, *J* = 8.59 Hz, 1H), 6.98 (d, *J* = 3.03 Hz, 1H), 6.92 (dd, *J* = 2.53, 8.59 Hz, 1H), 6.80 (ddd, *J* = 6.57, 10.48, 16.80 Hz, 1H), 6.21 (d, *J* = 16.67 Hz, 1H), 6.03 (d, *J* = 5.56 Hz, 1H), 5.74 (dd, *J* = 4.55, 10.61 Hz, 1H), 4.67 (spt, *J* = 6.06 Hz, 1H), 4.49-4.59 (m, 0.5H), 4.25-4.37 (m, 0.5H), 4.14-4.23 (m, 0.5H), 3.89-4.05 (m, 1.5H), 3.11-3.23 (m, 1H), 2.83-2.98 (m, 1H), 2.12 (s, 3H), 2.02-2.10 (m, 1H), 1.88 (dt, *J* = 3.66, 13.39 Hz, 1H), 1.49-1.82 (m, 2H), 1.35 (d, *J* = 6.06 Hz, 6H).

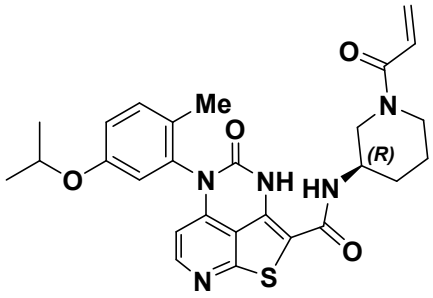

Compound 15: (*R*)-*N*-(1-Acryloylpiperidin-3-yl)-5-(5-isopropoxy-2-methylphenyl)-4-oxo-4,5-dihydro-3*H*-1-thia-3,5,8-triazaacenaphthylene-2-carboxamide. Compound 13 was prepared using general method 1. MS (ESI): mass calcd. for $C_{27}H_{30}N_5O_4S$ $[M+H]^+$, 520.20; m/z found, 520.1. ^1H NMR (600 MHz, CD_3OD): δ 8.34–8.28 (d, *J* = 5.6 Hz, 1H), 7.37–7.31 (d, *J* = 8.5 Hz, 1H), 7.04–6.99 (m, 1H), 6.96–6.91 (d, *J* = 2.8 Hz, 1H), 6.84–6.74 (m, 1H), 6.25–6.16 (m, 1H), 6.05–6.01 (m, 1H), 5.77–5.70 (m, 1H), 4.63–4.56 (m, 1H), 4.55–4.26 (m, 1H), 4.22–3.92 (m, 2H), 3.23–3.14 (m, 1H), 2.99–2.85 (m, 1H), 2.11–2.05 (s, 4H), 1.92–1.83 (m, 1H), 1.81–1.68 (m, 1H), 1.65–1.49 (m, 1H), 1.32–1.29 (s, 6H).

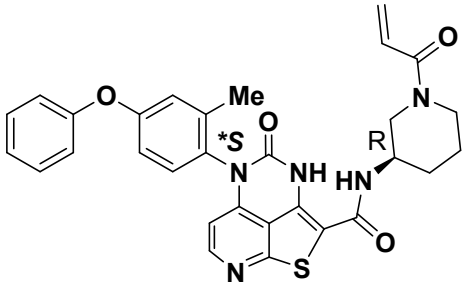

Compound 17: (*R*)-*N*-(1-Acryloylpiperidin-3-yl)-5-(**S*)-(2-methyl-4-phenoxyphenyl)-4-oxo-4,5-dihydro-3*H*-1-thia-3,5,8-triazaacenaphthylene-2-carboxamide. Compound 17 was prepared using general method 2. MS (ESI): mass calcd. for $C_{30}H_{28}N_5O_4S$ $[M+H]^+$, 554.19; m/z found, 554.5. ^1H NMR (400 MHz, DMSO-d_6): δ 10.29-10.20 (m, 1H), 8.37-8.32 (m, 1H), 8.13-8.04 (m, 1H), 7.50-7.35 (m, 3H), 7.25-7.17 (m, 1H), 7.17-7.07 (m, 3H), 7.02-6.95 (m, 1H), 6.87-6.73 (m, 1H), 6.16-6.06 (m, 1H), 6.03-5.97 (m, 1H), 5.72-5.64 (m, 1H), 4.54-4.18 (m, 1H), 4.10-3.95 (m, 1H), 3.84-3.74 (m, 1H), 3.17-2.92 (m, 1H), 2.82-2.62 (m, 1H), 2.07 (s, 3H), 2.00-1.88 (m, 1H), 1.84-1.74 (m, 1H), 1.74-1.61 (m, 1H), 1.51-1.36 (m, 1H).

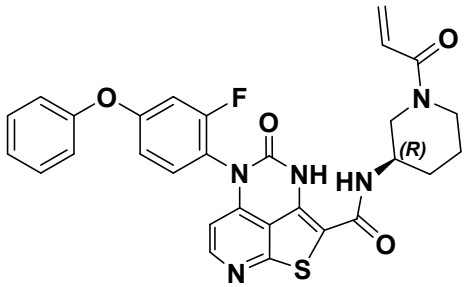

Compound 18: (*R*)-*N*-(1-Acryloylpiperidin-3-yl)-5-(2-fluoro-4-phenoxyphenyl)-4-oxo-4,5-dihydro-3*H*-1-thia-3,5,8-triazaacenaphthylene-2-carboxamide. Compound 18 was prepared using general method 3. MS (ESI): mass calcd. for $C_{29}H_{25}FN_5O_4S$, 558.16; m/z found, 558.2 $[M+H]^+$. ^1H NMR (400 MHz, DMSO-d_6): δ 10.37 (s, 1H), 8.33 (d, J = 5.4 Hz, 1H), 8.22-8.05 (m, 1H), 7.64-7.51 (m, 1H), 7.51-7.38 (m, 2H), 7.28-7.20 (m, 1H), 7.20-7.09 (m, 3H), 6.99-6.90 (m, 1H), 6.86-6.63 (m, 1H), 6.17 (d, J = 5.4 Hz, 1H), 6.07 (d, J = 16.6 Hz, 1H), 5.65 (d, J = 11.1 Hz, 1H), 4.53-4.07 (m, 1H), 4.08-3.88 (m, 1H), 3.84-3.65 (m, 1H), 3.11-2.91 (m, 1H), 2.78-2.56 (m, 1H), 2.00-1.83 (m, 1H), 1.80-1.69 (m, 1H), 1.68-1.54 (m, 1H), 1.47-1.30 (m, 1H).

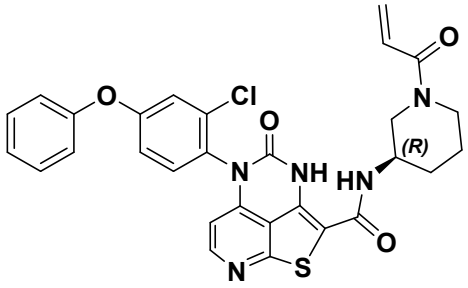

Compound 19: (*R*)-*N*-(1-Acryloylpiperidin-3-yl)-5-(2-chloro-4-phenoxyphenyl)-4-oxo-4,5-dihydro-3*H*-1-thia-3,5,8-triazaacenaphthylene-2-carboxamide. Compound 19 was prepared using general method 3. MS (ESI): mass calcd. for $C_{29}H_{25}ClN_5O_4S$ $[M+H]^+$, 574.13; m/z found, 574.3. ^1H NMR (400 MHz, CD3OD): δ 8.33 (d, J = 5.6 Hz, 1H), 7.78-7.73 (m, 1H), 7.52-7.45 (m, 1H), 7.36-7.21 (m, 2H), 7.10-7.02 (m, 2H), 7.00-6.88 (m, 2H), 6.88-6.70 (m, 1H), 6.28-6.14 (m, 1H), 6.07 (d, J = 5.6 Hz, 1H), 5.81-5.66 (m, 1H), 4.63-3.87 (m, 3H), 3.25-3.10 (m, 1H), 3.01-2.82 (m, 1H), 2.14 (s, 3H), 2.09-2.01 (m, 1H), 1.94-1.83 (m, 1H), 1.81-1.68 (m, 1H), 1.65-1.52 (m, 1H).

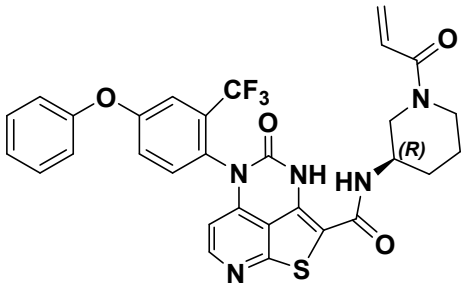

Compound 20: (*R*)-*N*-(1-Acryloylpiperidin-3-yl)-4-oxo-5-(4-phenoxy-2-(trifluoromethyl)phenyl)-4,5-dihydro-3*H*-1-thia-3,5,8-triazaacenaphthylene-2-carboxamide.

Compound 20 was prepared using general method 3. MS (ESI): mass calcd. for $C_{30}H_{25}F_3N_5O_4S$, 608.16 $[M+H]^+$; m/z found, 608.3. ^1H NMR (400 MHz, DMSO-d_6): δ 10.38 (s, 1H), 8.34 (d, J = 5.5 Hz, 1H), 8.20–8.02 (m, 1H), 7.74 (d, J = 8.7 Hz, 1H), 7.59–7.38 (m, 4H), 7.35–7.14 (m, 3H), 6.90-6.65 (m, 1H), 6.20-6.00 (m, 2H), 5.66 (d, J = 12.2 Hz, 1H), 4.52-4.12 (m, 1H), 4.10-3.89 (m, 1H), 3.84-3.63 (m, 1H), 3.16–2.88 (m, 1H), 2.83–2.55 (m, 1H), 2.05-1.85 (m, 1H), 1.85–1.51 (m, 2H), 1.50-1.30 (m, 1H).

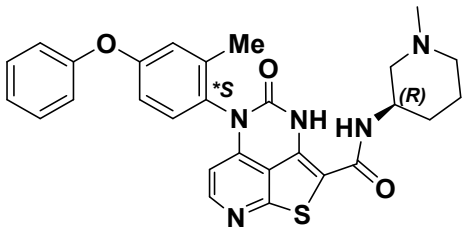

Compound 21: (*R*)-5-(**S*)-(2-Methyl-4-phenoxyphenyl)-*N*-(1-methylpiperidin-3-yl)-4-oxo-4,5-dihydro-3*H*-1-thia-3,5,8-triazaacenaphthylene-2-carboxamide. To a stirred suspension of 5-(**S*)-(2-methyl-4-phenoxyphenyl)-4-oxo-4,5-dihydro-3*H*-1-thia-3,5,8-triazaacenaphthylene-2-carboxylic acid (150 mg, 0.359 mmol) was added (*R*)-1-methylpiperidin-3-amine (81 mg, 0.54 mmol), HATU (164 mg, 0.43 mmol), DIEA (0.15 mL, 1.077 mmol), and DMF (3 mL). The resulting mixture was stirred at room temperature overnight, then purified by HPLC (MeOH/H_2O), yielding the title compound as a yellow solid (102 mg, 55%). MS (ESI): mass calcd. for $C_{28}H_{28}N_5O_3S$, 514.19 $[M+H]^+$; m/z found, 514.2. ^1H NMR (400 MHz, CD_3OD): δ 8.30 (d, J = 5.6, 1H), 7.43-7.35 (m, 2H), 7.31-7.26 (m, 1H), 7.20-7.14 (m, 1H), 7.12-7.08 (m, 2H), 7.08-7.03 (m, 1H), 7.01-6.95 (m, 1H), 6.05 (d, J = 5.6, 1H), 4.24-4.11 (m, 1H), 3.02-2.90 (m, 1H), 2.78-2.68

(m, 1H), 2.36 (s, 3H), 2.29-2.16 (m, 2H), 2.12 (s, 3H), 1.95-1.78 (m, 2H), 1.74-1.63 (m, 1H), 1.57-1.45 (m, 1H).

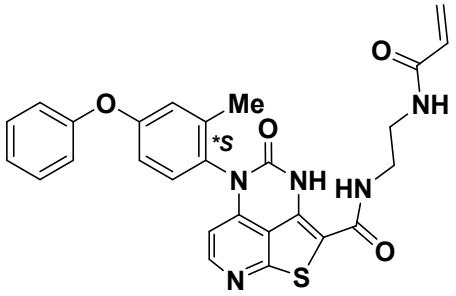

Compound 25: *N*-(2-Acrylamidoethyl)-5-(**S*)-(2-methyl-4-phenoxyphenyl)-4-oxo-4,5-dihydro-3*H*-1-thia-3,5,8-triazaacenaphthylene-2-carboxamide. Compound 25 was prepared using general method 3. MS (ESI): mass calcd. for $C_{27}H_{24}N_5O_4S$, 514.15 $[M+H]^+$; m/z found, 514.1. ^1H NMR (400 MHz, CD_3OD) δ 8.31-8.20 (m, 1H), 7.42-7.35 (m, 2H), 7.30-7.23 (m, 1H), 7.19-7.14 (m, 1H), 7.10-7.02 (m, 3H), 6.99-6.93 (m, 1H), 6.28-6.19 (m, 2H), 6.06-5.98 (m, 1H), 5.68-5.61 (m, 1H), 3.53-3.45 (m, 4H), 2.11 (s, 3H).

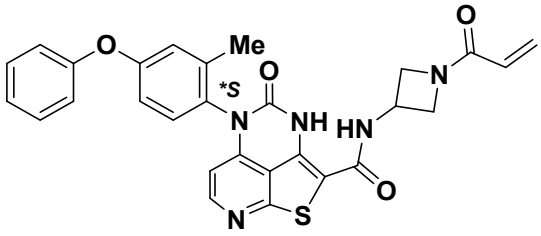

Compound 26: *N*-(1-Acryloylazetidin-3-yl)-5-(**S*)-(2-methyl-4-phenoxyphenyl)-4-oxo-4,5-dihydro-3*H*-1-thia-3,5,8-triazaacenaphthylene-2-carboxamide. Compound 26 was prepared using general method 3. MS (ESI): mass calcd. for $C_{28}H_{24}N_5O_4S$, 526.15 $[M+H]^+$; m/z found, 526.1. ^1H NMR (400 MHz, DMSO-d_6 and CD_3OD): δ 8.29 (d, J = 5.5 Hz, 1H), 7.43-7.33 (m, 2H), 7.31-7.23 (m, 1H), 7.17-7.09 (m, 1H), 7.08-6.98 (m, 3H), 6.97-6.89 (m, 1H), 6.37-6.23 (m, 1H), 6.20-6.08 (m, 1H), 5.98 (d, J = 5.5 Hz, 1H), 5.71-5.60 (m, 1H), 4.81-4.69 (m, 1H), 4.58-4.47 (m, 1H), 4.24-4.17 (m, 2H), 4.04-3.97 (m, 1H), 2.04 (s, 3H).

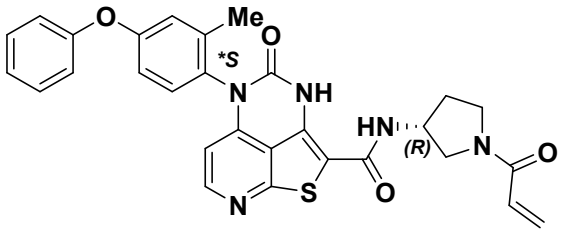

Compound 27: (*R*)-*N*-(1-Acryloylpyrrolidin-3-yl)-5-(**S*)-(2-methyl-4-phenoxyphenyl)-4-oxo-4,5-dihydro-3*H*-1-thia-3,5,8-triazaacenaphthylene-2-carboxamide. To a round bottom flask were added 5-(**S*)-(2-methyl-4-phenoxyphenyl)-4-oxo-4,5-dihydro-3*H*-1-thia-3,5,8-triazaacenaphthylene-2-carboxylic acid (200 mg, 0.48 mmol), DMF (5 mL), HATU (237 mg, 0.62 mmol), and DIEA (155 mg, 1.2 mmol) and allowed to stir. After 5 minutes, (*R*)-1-(3-aminopyrrolidin-1-yl)prop-2-en-1-one (169 mg, 0.96 mmol) was added portion wise and the mixture was stirred for 1 hour. The reaction was quenched with H_2O and the ppt was filtered and dried. The resulting solid was purified by FCC (SiO_2, EtOAc/hexanes)to give the title compound as a white solid (83 mg, 32%). HRMS calculated for $C_{29}H_{26}N_5O_4S$ 540.1706, found 540.1701. ^{1}H NMR (400 MHz, DMSO-d_6): δ 10.24 (s, 1H), 8.43-8.22 (m, 2H), 7.57–7.29 (m, 3H), 7.25-7.04 (m, 4H), 7.03-6.90 (m, 1H), 6.70-6.45 (m, 1H), 6.13 (d, *J* = 16.4 Hz, 1H), 6.05-6.88 (m, 1H), 5.73-5.57 (m, 1H), 4.60-4.30 (m, 1H), 3.91–3.36 (m, 4H), 2.24–1.89 (m, 5H).

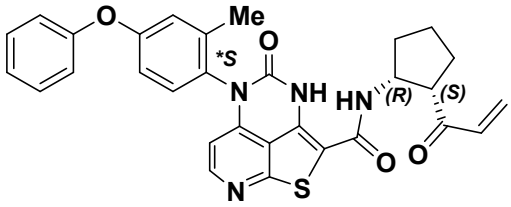

Compound 29: *N*-((1*R*,2*S*)-2-Acrylamidocyclopentyl)-5-(**S*)-(2-methyl-4-phenoxyphenyl)-4-oxo-4,5-dihydro-3*H*-1-thia-3,5,8-triazaacenaphthylene-2-carboxamide. Compound 29 was prepared using general method 3. MS (ESI): mass calcd. for $C_{30}H_{28}N_5O_4S$ $[M+H]^+$ 554.19; m/z found, 554.5. ^{1}H NMR (400 MHz, CD_3OD): δ 8.30 (d, *J* = 5.6 Hz, 1H), 7.44-7.33 (m, 2H), 7.30-7.24 (m, 1H), 7.20-7.13 (m, 1H), 7.12-7.02 (m, 3H), 7.00-6.92 (m, 1H), 6.31-6.14 (m, 2H), 6.04 (d, *J* = 5.6 Hz, 1H), 5.65-5.56 (m, 1H), 4.48-4.33 (m, 2H), 2.17-2.03 (m, 5H), 1.95-1.85 (m, 1H), 1.80-1.60 (m, 3H).

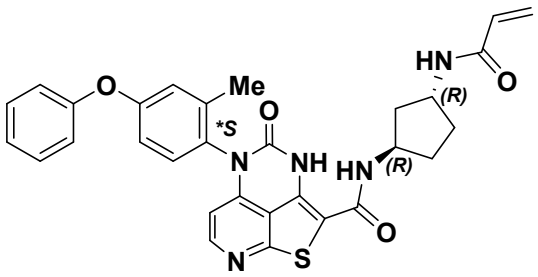

Compound 30: *N*-((1*R*,3*R*)-3-Acrylamidocyclopentyl)-5-(**S*)-(2-methyl-4-phenoxyphenyl)-4-oxo-4,5-dihydro-3*H*-1-thia-3,5,8-triazaacenaphthylene-2-carboxamide. Compound 30 was prepared using general method 3. MS (ESI): mass calcd. for $C_{30}H_{28}N_5O_4S$ $[M+H]^+$, 554.19; m/z found, 554.4. ^1H NMR (400 MHz, CD_3OD): δ 8.31 (d, J = 5.6 Hz, 1H), 7.43-7.35 (m, 2H), 7.33-7.24 (m, 1H), 7.18-7.12 (m, 1H), 7.12–7.01 (m, 3H), 6.99-6.90 (m, 1H), 6.26–6.18 (m, 2H), 6.06 (d, J = 5.6 Hz, 1H), 5.68-5.55 (m, 1H), 4.57–4.45 (m, 1H), 4.44–4.30 (m, 1H), 2.28-2.14 (m, 2H), 2.11 (s, 3H), 2.04-1.86 (m, 2H), 1.73–1.45 (m, 2H).

Assay conditions

*BTK Binding Assay***.** Recombinant, unphosphorylated-BTK (UP-BTK) kinase domain was purchased from Proteros GmbH (Munich, Germany). Eu-anti-GST antibody, kinase buffer, and Alexa-Fluor 647-labeled kinase tracer were purchased from Invitrogen (Carlsbad, CA).

To determine the binding affinity for each compound, a BTK kinase Lanthascreen assay was utilized to monitor compound binding to UP-BTK by competing with a fluorescent-labeled tracer. Titrations of compound in DMSO were added to 384-well plates, followed in succession by 2.67 nM UP-BTK, 2.0 nM detection antibody, and 50 nM tracer in kinase buffer. The plates were incubated for 1 hr at room temperature and fluorescence read on Infinite F500 from Tecan.

Emission ratio (ER) was calculated by dividing the reading at 665 nm by the reading at 615 nm. Inhibition rate (IR%) was determined by the following equation: IR% = $(ER_{high} - ER_{compound})$ x 100 / $(ER_{high} - ER_{low})$, where ER_{high}, ER_{low}, and $ER_{compound}$ refer to the emission ratio of the high control (no compound), low control (no enzyme), and compound treated wells, respectively. The IC_{50} for each compound was then calculated from the IR% of the titrations using a four-parameter logistic regression (4-PL) fit.

Determination of inhibitor potency (k_{inact}/K_I ratios). Full-length BTK enzyme was purchased from Carnabio USA (Natick, MA). Srctide (NH2-KKKAPFSWYLPEEG) was purchased from Anaspec (Fremont, CA). ATP, phosphoenolpyruvate, nicotinamide adensine dinucleotide reduced form (NADH), pyruvate kinase/lactic dehydrogenase (PK/LDH), $MgCl_2$, tris(2-carboxyethyl)phosphine (TCEP) and pluronic F127 were purchased from Sigma. 1 M Hepes-NaOH (pH 7.5) and Tween-20 were purchased from Teknova and Enzo, respctively. Transparent 384-well plates were purchased from Greiner. To determine k_{inact}/K_I ratio for each compound, BTK reaction progress at each compound concentration was monitored by using PK/LDH assay, which couples adenosine

diphosphate (ADP) production from kinase activities to oxidation of NADH.[28] Assays were performed in transparent 384-well plates in the assay mixture containing 50 mM Hepes-NaOH (pH 7.5), 10 mM $MgCl_2$, 0.24 mM ATP, 0.45 mM srctide (NH2-KKKAPFSWYLPEEG), 0.50 mM phosphoenolpyruvate, 0.30 mM NADH, 12-20 U/mL pyruvate kinase, 18-28U/mL lactic dehydrogenase, 0.002% Tween-20, 1mM TCEP, and 0.01% Pluronic F127, and the indicated concentrations of inhibitor (or DMSO). Reactions were initiated by the addition of 1 nM full-length BTK enzyme and the final concentration of DMSO was kept at 0.1%. The substrate concentrations for the assay were at the K_M value and 3-times of the K_M value for ATP and the peptide substrates, respectively. Background reactions without the BTK enzyme were subtracted from all reactions with the enzyme. Reaction time courses were monitored at RT by recording absorbance at 340 nm for 2 hours with readings taken 2-min intervals on Tecan Spark microplate reader (Tecan U. S., Morrisville, NC) equipped with SparkControl software. The reaction progress curves corresponding to the linear range of the DMSO control for 2 hours were fit to eq 1:

$$\text{Product} = \frac{V_0}{k_{obs}} [1\text{-}\exp(-k_{obs}t)] \qquad (1)$$

where V_o is the initial rate and t is time, to obtain the first order rate constant for enzyme inactivation (k_{obs}) at each inhibitor concentration. The k_{obs} values were then plotted versus inhibitor concentration ([I]) and fit to eq 2:

$$k_{obs} = \frac{k_{inact}[I]}{K_I + [I]} \qquad (2)$$

where k_{inact} is the maximal rate of inactivation and K_I is the inhibitor concentration that yields half the rate of maximal inactivation. The k_{inact} and K_I values determined were used to calculate the overall potency

k_{inact}/K_I ratios.[23] For highly potent compounds with K_I values close to or less than the enzyme concentration (1 nM), assays were performed again at higher ATP concentration (4.8 mM, which is 20-fold of the K_M value) to ensure more accurate determination of potency. K_I at 0.24 mM ATP was then calculated by dividing the apparent K_I at 4.8 mM ATP by 10.5.

Determination of rotational interconversion barriers $\Delta G^{\ddagger}_{rot}$. [29] Resolved atropisomers were heated in aqueous ethanol and the appearance of the alternate atropisomers were quantified by chiral SFC with UV detection at 254.4 nm. The rate constants for racemization were determined from the relative quantities of the two atropisomers as a function of time according to equation 3.

$$k = \frac{1}{2}\frac{d\ln\left(\frac{1+D:L}{1-D:L}\right)}{dt}. \qquad (3)$$

The rotational energy barriers $\Delta G^{\ddagger}_{rot}$ were calculated from the rate constants for racemization according to equation 4.

$$k = Ae^{-\Delta G\ddagger rot/RT} \qquad (4)$$

Covalent adduct assay. In this assay, recombinant purified BTK kinase domain (Proteros) is reacted to completion with the inhibitor. Aliquots of the reaction are then run over a C18 reversed phase HPLC column (Phenomenex Aeris Widepore, 50 x 2.1 mm, 3.6 um) under non-denaturing (native) conditions and under denaturing conditions (8M urea, 70 °C) using an Agilent 1290 uHPLC system with dual column setup. The HPLC is coupled to an Agilent 6550 qTOF mass spectrometer to enable precise identification of free protein and adduct by mass. The area under

the peak of the resulting chromatogram is proportional to the amount of detected protein and is used to calculate the percentage of free and modified BTK.

Mouse CD69 Primary Cell Assay. Anti-mouse IgM was purchased from Jackson ImmunoResearch (West Grove, PA). Mouse CD19-APC and mouse CD69-FITC antibodies were purchased from BD Pharmingen (San Diego, CA).

To determine the potency of each compound, inhibition of anti-IgM-induced B cell activation in mouse primary cells was assessed by flow cytometry. Mouse splenocytes were prepared from C57Bl/6 mice into complete culture media (RPMI 1640, 10% fetal bovine serum, 2 mM Glutamax (Gibco)) and seeded at a density of 2 x 10^6 cells/mL, followed by a 1 hour incubation with a titration of compound in DMSO and overnight incubation with anti-IgM (5 μg/mL in media). Cells were then collected by centrifugation and stained with fluorescent antibodies against CD19 and CD69 for 30 minutes, washed, fixed (1% paraformaldehyde), and acquired on FACSCalibur or FACSCanto II (BD Biosciences).

Each sample was gated on forward and side scatter for lymphocytes and on CD19+ for B cells. The percentage of activated B cells was defined as the proportion of CD19+CD69+ cells over total CD19+ cells.

Rat Whole Blood Assay. Anti-rat IgD was purchased from AbD Serotec (Oxford, United Kingdom). Rat B220-PE and rat CD86-FITC were purchased from eBioscience (San Diego, CA). Lysing buffer was purchased from BD Biosciences (San Diego, CA).

To determine the potency of each compound, inhibition of anti-IgD-induced activation of B cells in rat whole blood was assessed by flow cytometry. Heparinized blood was collected from Wistar rats, supplemented with penicillin (100 U/mL) and streptomycin (100 μg/mL), and incubated for

1 hour with a titration of compound in DMSO (0.3% final concentration). The blood was then stimulated and incubated overnight at 37 °C with anti-IgD (10 μg/mL). The samples were then stained with fluorescent antibodies against CD86 and B220 for 30 minutes, red blood cells removed with lysing buffer, washed, fixed, and acquired on FACSCalibur.

Each sample was gated on forward and side scatter for lymphocytes and on B220+ for B cells. The percentage of activated B cells was defined as the proportion of B220+CD86+ cells over total B220+ cells.

Inhibition percentage was determined by the following equation: Inhibition% = ($ActB_{stim}$ – $ActB_{compound}$) x 100 / ($ActB_{stim}$ – $ActB_{unstim}$), where $ActB_{high}$, $ActB_{unstim}$, and $ActB_{compound}$ refer to the percentage of activated B cells of the stimulated (no compound), unstimulated (no antibody), and compound treated wells, respectively. The IC_{50} for each compound was then calculated from the inhibition % of the titrations using a 4-PL fit.

Human whole blood assay. 160 μL of human whole blood was incubated with 20 μL of titrated compounds for 30-60 minutes and stimulated for 18 hours with 20 μL of anti-IgM (30 μg/mL, Jackson ImmunoResearch) at 37°C. Test compounds were tested in duplicate during each IC_{50} determination. The next day, the cells were stained for 1 hour with fluorescent antibodies to CD19 and CD69 (R&D). The red blood cells were lysed (buffer EL, Qiagen) and the samples read using a FACSC anto II (BD). Graphpad Prism 5, version 5.01, was used to generate a concentration response curve and IC_{50} values.

Inhibition percentage was determined by the following equation: Inhibition% = ($ActB_{stim}$ – $ActB_{compound}$) x 100 / ($ActB_{stim}$ – $ActB_{unstim}$), where $ActB_{high}$, $ActB_{unstim}$, and $ActB_{compound}$ refer to the percentage of activated B cells of the stimulated (no compound), unstimulated (no antibody),

and compound treated wells, respectively. The IC_{50} for each compound was then calculated from the inhibition % of the titrations using a 4-PL fit.

Liver Microsomal Metabolic Stability Assay. The liver microsomal metabolic stability assay was conducted at Cyprotex. The microsomes used for metabolic stability studies were as follows: human liver microsomes (pooled male and female), rat liver microsomes (pooled male Sprague Dawley rats), mouse liver microsomes (pooled male CD mice), dog liver microsomes (male beagle), and monkey liver microsomes (male cynomolgus). Microsomes (final protein concentration 0.5 mg/mL), 0.1 M phosphate buffer pH 7.4 containing 1 mM $MgCl_2$ and test compound (final substrate concentration 1 μM; final DMSO concentration 0.05 %) were pre-incubated at 37 °C prior to the addition of NADPH (final concentration 1 mM) to initiate the reaction. At 6 time points (0, 5, 10, 20, 40 and 60 min) reactions were stopped by the removal of 50 μL of the incubation mixture into methanol. The incubation plates were centrifuged at 2,500 rpm for 20 min at 4 °C to precipitate the protein. Following protein precipitation, the sample supernatants were combined in cassettes of up to 8 compounds and analyzed using LC-MS/MS conditions.

The compound half-lives were derived from plots of the ln of percent remaining compound over time to determine the intrinsic clearance. The predicted hepatic clearance was derived from the intrinsic clearance value using equations from the well-stirred model, where no correction was made for plasma protein or liver microsomal binding and the blood to plasma concentration ratio was assumed to be one. The extraction ratio (ER) was calculated by dividing the predicted hepatic clearance by species blood flow (Q), where Q is 150, 70, 31, 44, and 21 mL/min/kg for mouse, rat, dog, monkey and human, respectively.

Pharmacokinetic Studies. Compound **27** was formulated in 20% HP-β-CD to prepare a 1 mg/mL solution.

Rat pharmacokinetic studies were conducted by Biodura, Shanghai. Separate cohorts (n=3) of non-fasted male Sprague Dawley rats were administered compound **27** at a dose of 1 mg/kg IV or 5 mg/kg PO as a solution. Blood samples were collected at 0.033 (IV only), 0.083 (IV only), 0.25, 0.5, 1, 2, 4, 8, and 24 h post dose after administration via the jugular vein catheter. Blood samples were collected into tubes containing K_2EDTA and placed on wet ice. The plasma fraction was separated by centrifugation and kept frozen at -20 °C. Concentrations of compound **27** in plasma were determined using a qualified liquid chromatography-triple quadrupole mass spectrometry (LC-MS/MS) method with a limit of quantification (LOQ) of 1 ng/mL.

Dog pharmacokinetic studies were conducted internally at Janssen Research & Development. Six male beagle dogs were fasted overnight prior to dosing and food was withheld through the first 4 hours of blood sample collection. Compound **27** was administered to the IV cohort (n = 3) via a single IV bolus dose of 0.5 mg/kg and to the PO cohort (n = 3) orally via stomach intubation with a dose of 2.5 mg/kg. Blood samples were collected at pre-dose, 0.033 (IV only), 0.083 (IV only), 0.25, 0.5, 1, 2, 4, 7, and 24 h post dose. Blood samples (~1 mL) were obtained from the jugular or cephalic veins, collected into tubes containing K_2EDTA, and placed on wet ice. The samples were centrifuged and the resulting plasma was separated and stored frozen at –70 °C. Concentrations of compound **27** in plasma were determined using a qualified liquid chromatography-triple quadrupole mass spectrometry (LC-MS/MS) assay with a LOQ of 1 ng/mL.

Pharmacokinetic parameter values were derived from noncompartmental analysis of the plasma concentration versus time data using Phoenix WinNonlin software (Certara, Princeton, NJ). Half-life was not reported if <3 data points were used to define the terminal phase.

In vivo BTK occupancy. Compound **27** or vehicle (20% HPβCD) was administered orally to female Wistar rats (approximately 154-170 g at time of study), and blood was obtained into heparinized tubes by retroorbital bleeding at 2, 4, 8, 24, 32, and 48 hours after dosing. Half of each sample was prepared into plasma by centrifugation (5000 rpm for 10 min in 4 °C) and compound levels measured by LC/MS. The other half was used to assess BTK protein occupancy by ELISA. Cell lysates were prepared from the blood, and free BTK protein was tagged by a biotinylated probe which was then captured on the surface of a streptavidin-coated microtiter plate and detected by ELISA using an antibody specific for BTK (BD Transduction). Percent free BTK was calculated by dividing the background adjusted optical densities of samples from rats administered compound **27** by samples from rats administered vehicle. Percent BTK occupancy was defined as 100% minus percent free BTK.

Collagen induced arthritis model. Female Wistar rats (Shanghai SLAC Laboratory Animal Co Ltd) were approximately 133-163 g (6-8 weeks of age) at initiation of dosing. Hydroxypropyl-β-cyclodextrin (HPβCD; 20% w/v) solution was prepared in distilled water, adjusted pH to 2.1 with 6 M HCl and used as the vehicle. YiSaiPu, a recombinant human Tumor Necrosis Factor-α Receptor II: IgG Fc fusion protein was used as a control (Lot: 201405038/201407028) (Shanghai CP Guojian Pharmaceutical Co., Ltd., Shanghai, P.R.China). Collagen from bovine cartilage, Type II (CII) (Chondrex; Redmond, WA, USA) and Incomplete Freund's adjuvant (IFA) (Sigma-Aldrich, St. Louis, MO, USA) was used to initiate disease. Type II collagen was dissolved at a concentration of 2 mg/mL in 100 mM acetic acid by stirring at 4 °C overnight. A high-speed homogenizer (28,000 rpm, FLUKO Equipment Shanghai Co., Ltd) was used to emulsify the 2 mg/mL CII solution in an equal volume of the IFA on ice for 3 min.

Arthritis was induced by intradermal injection of CII in IFA.[30] 104 rats were used in the study. Before immunization, 6 rats were randomly selected as a naïve group. The other 98 rats were anesthetized with inhalational isoflurane and injected intradermally at the base of the tail with 0.2 mL of the emulsion (1 mg/mL CII/IFA), 2-3 cm from the body on day 0 and day 7. On day 9, out of the 98 rats that were immunized, the 48 rats with the most developed arthritis based on paw volume measurements were divided into 6 groups (n=8) with a stratified random block design according to average hind paw volume of each rat. Vehicle or different doses of compound **24** were administered QD (once a day) from day 9 to day 16; anti-TNF was administered QOD (once every other day) on days 9, 11, 13, and 15. Left and right hind paw volumes were measured by a Plethysmometer (Catalog No. 7140, Ugo Basile. Italy) and body weight was monitored daily for 7 consecutive days after initiation of test article dosing.

T Cell IL-2 Assay. An IL-2 ELISA assay was developed to assess the activity of BTK inhibitors in human T cells. The assay uses anti-CD3 and anti-CD28 antibodies to trigger general T cell activation. A cytokine, IL-2, produced during T cell activation was measured using an ELISA assay.

Briefly, 90 µL of human CD4+ T cells were incubated with 10 µL of titrated compounds for 30-60 minutes and stimulated for 18 hours with 10 µL of anti-CD3 (1 µg/mL, BD) and anti-CD28 (1 µg/mL, eBioscience) at 37°C. JNJ-64264681 was tested in duplicate during each IC_{50} determination. The next day, the supernatant was collected and the concentration of IL-2 was determined with an ELISA assay. An ITK inhibitor was included as a positive control in all experiments.

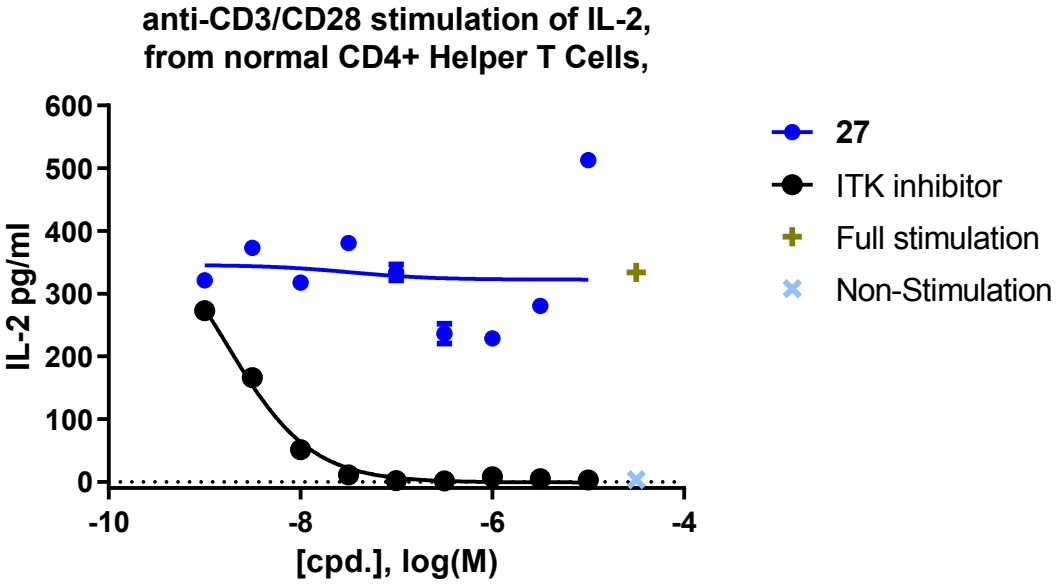
anti-CD3/CD28 stimulation of IL-2,
from normal CD4+ Helper T Cells,
IL-2 pg/ml
600
500
400
300
200
100
0
-10
-8
-6
-4
[cpd.], log(M)
27
ITK inhibitor
Full stimulation
Non-Stimulation